DEPARTMENT OF TRANSPORTATION

Investigation on Mix Design of Recycled Asphalt Pavement (RAP) Materials

Jia-Liang Le, Principal Investigator

Department of Civil, Environmental, and Geo- Engineering
University of Minnesota

May 2026

Research Report
Final Report 2026-21

LOCAL ROAD RESEARCH BOARD

To get this document in an alternative format or language, please call 651-366-4720 (711 or 1-800-627-3529 for MN Relay). You can also email your request to ADArequest.dot@state.mn.us. Please make your request at least two weeks before you need the document.

Technical Report Documentation Page

1. Report No.	2.	3. Recipients Accession No.	
MN 2026-21			
4. Title and Subtitle Investigation on Mix Design of Recycled Asphalt Pavement (RAP) Materials		5. Report Date May 2026 6.	
7. Author(s) Jia-Liang Le, Mihai Marasteanu, Mugurel Turos, Zifeng Zhao, and Shambhavi Khanal		8. Performing Organization Report No.	
9. Performing Organization Name and Address Department of Civil, Environmental, and Geo Engineering University of Minnesota 500 Pillsbury Dr SE, Minneapolis, MN 55455		10. Project/Task/Work Unit No. #2024004 11. Contract (C) or Grant (G) No. (c) 1036342 (wo) 82	
12. Sponsoring Organization Name and Address Minnesota Department of Transportation Office of Research & Innovation 395 John Ireland Boulevard, MS 330 St. Paul, Minnesota 55155-1899		13. Type of Report and Period Covered Final report 14. Sponsoring Agency Code	
15. Supplementary Notes https://mdl.mndot.gov/			

16. Abstract (Limit: 250 words)

Recycled asphalt pavement (RAP) is widely used in asphalt mixture production because it reduces material cost, conserves natural resources, and improves sustainability in pavement construction. However, increasing RAP content can also introduce compactability issues and weak cracking resistance. For this reason, a better understanding of RAP material characteristics and mixture behavior is needed to support reliable mixture design and implementation. This project investigates the mix design, compaction behavior, and low-temperature mechanical performance of RAP mixtures, with additional evaluation of graphite nanoplatelet (GNP) modification. The work includes a literature review on RAP compaction and design, followed by RAP characterization using processed black and white curves, chunk index, gradation, moisture content, and binder content. A gradation-based mix design procedure is developed to prepare mixtures containing 25%, 40%, and 50% RAP. Gyratory compaction testing shows that, under the laboratory conditions used in this study, mixtures with higher RAP contents reach the target air void level with fewer gyrations. Additional testing shows that adding 6% GNP by weight of fresh binder moderately improves compaction and reduces gyration demand, although the benefit becomes limited at lower compaction temperature. Low-temperature semi-circular bend and bending beam rheometer tests indicate that RAP mixtures had fracture energy comparable to the virgin mixture and generally higher apparent fracture toughness and flexural strength. Overall, the results indicate that RAP mixtures designed and prepared under the conditions used in this study can achieve satisfactory compactability and low-temperature performance, supporting the feasibility of using higher RAP contents in asphalt mixtures.

17. Document Analysis/Descriptors	18. Availability Statement		
Recycled materials, Asphalt mixtures, Mix design, Low temperature tests, Graphite	No restrictions. Document available from: National Technical Information Services, Alexandria, Virginia 22312		
19. Security Class (this report) Unclassified	20. Security Class (this page) Unclassified	21. No. of Pages 64	22. Price

Investigation on Mix Design of Recycled Asphalt Pavement (RAP) Materials

Final Report

Prepared by:

Jia-Liang Le
Mihai Marasteanu
Mugurel Turos
Zifeng Zhao
Shambhavi Khanal
Department of Civil, Environmental, and Geo- Engineering
University of Minnesota

May 2026

Published by:

Minnesota Department of Transportation
Office of Research & Innovation
395 John Ireland Boulevard, MS 330
St. Paul, Minnesota 55155-1899

Acknowledgements

The authors gratefully acknowledge the financial support provided by the Minnesota Department of Transportation and Minnesota Local Road Research Board.

Special acknowledgements go to the project champion, Eddie Johnson, for his guidance and technical support provided over the entire duration of the research investigation.

Thank you to the members of this project's Technical Advisory Panel: Brandon Brever, Juan Pinero, Tim Plath, Michael Skurdalsvold, Marcus Bekele, and Julie Swiler.

We also acknowledge the continuous logistical support provided by Project Coordinator Jiran Jackie, which was instrumental in successfully completing this project.

Table of Contents

List of Figures

List of Tables

Executive Summary

Recycled asphalt pavement (RAP) materials are increasingly used in asphalt pavement construction. Their use offers several benefits, including reduced costs and environmental impacts, as well as decreased demand for virgin aggregates and asphalt binders. Although extensive research has examined the mechanical performance of RAP materials, comparatively little attention has been given to their compaction properties. Compaction plays a critical role in determining the mechanical properties and durability of asphalt mixtures; therefore, understanding the compaction behavior of RAP is essential for developing reliable mix designs.

To address this knowledge gap, this study presents an investigation of: (1) the effect of RAP content on compaction performance through a gyratory compaction test; (2) the influence of graphene nanoplatelet (GNP) addition on RAP compaction through a gyratory compaction test; and (3) the strength, fracture, and creep properties of RAP mixtures with varying RAP contents and GNP modifications through semi-circular bend tests and bending beam rheometer tests.

The results provide insights into RAP mix design, particularly regarding the potential to increase RAP content, which carries important implications for both pavement construction and environmental sustainability.

Chapter 1: Introduction

Recycled asphalt pavement (RAP) materials have increasingly seen more applications in the construction of asphalt pavements. In 2016, MnDOT published a synopsis on the use of RAP material (MnDOT 2016). The synopsis identified various benefits of using the RAP materials, which include the reduction of cost and environmental impacts and the demand of virgin aggregates and asphalt binders. MnDOT has a long history of incorporating RAP into plant mixed asphalt.

It has been widely recognized that one of the most important considerations in the design of asphalt mixtures is the gradation of aggregates. The proper choice of the gradation has important implications for the compaction performance, which in turn affects the mechanical properties and durability of the constructed pavements. Recent studies by the PI and co-PI on Superpave 5 showed that, by properly choosing the gradation according to the maximum density line, one can improve the compaction performance considerably (Yan et al. 2022). However, similar investigations focused on the gradation of the RAP used in mix design have not been performed. Meanwhile, previous work by the team also showed the improvements in the compaction properties and mechanical properties of the asphalt mixtures by adding graphite nanoplatelet (GNP) to the binders (Le et al. 2020).

In this study, we perform a systematic experimental investigation on the compaction and mechanical properties of RAP mixes. The compaction experiments involve laboratory gyratory compaction on RAP mixes with different RAP contents. To facilitate this investigation, a mix design method i developed for RAP materials. The measured compaction curves are used to evaluate the compaction performance of RAP materials. The second part of compaction experiments involve RAP mixes modified by GNP, whose content is calculated based on the fresh binder. The last part of this investigation focuses on strength, fracture, and creep experiments on different RAP mixes at low temperatures.

The report's organization is as follows: Chapter 2 provides a summary of previous literature; Chapter 3 describes the compaction experiments on the conventional RAP mixes; Chapter 4 presents the compaction experiments on the RAP mixes modified by GNP; Chapter 5 presents the results of strength, fracture, and creep tests on different RAP mixes, and Chapter 6 presents a final discussion on the analysis presented in this report.

Chapter 2: Literature Review

The use of recycled materials is common practice in the production of asphalt mixtures for pavement applications. The use of Reclaimed Asphalt Pavement (RAP) has significantly increased over the years due to considerable economic benefits and reduction in environmental impact. Most, if not all, asphalt mixtures placed down in the past decade contains different amount of RAP, and this amount has increased over the years with the development of "rejuvenating" additives that are used to counteract the detrimental effect of the aged and oxidized binder present in RAP on the mechanical properties of asphalt mixtures.

Most of the research efforts investigating the use of RAP have focused on the effect of the aged binder on the mechanical and rheological properties of asphalt mixtures. Very few efforts were dedicated to studying the link between the use of RAP and the compaction properties of asphalt mixtures.

This chapter provides a review of the existing knowledge on compaction of RAP materials . The review will start with general information about the compaction process and the main factors responsible for achieving target density values. The review will continue with research efforts in which specific factors, related to RAP materials characterization, were investigated to understand their effect on compaction.

2.1 Compaction of Asphalt Mixtures

Compaction of asphalt mixtures has a significant effect on pavements performance, and affects all major distresses commonly observed in asphalt pavements (Finn and Epps 1980, Linden et al. 1989, Vivar and Haddock 2006, Willoughby and Mahoney 2007). Improving compaction results in significant improvements in durability. The compaction of mixture is controlled by two key factors: the compactability of mixture as a result of mix design, and field compaction operations. In this review we address only the studies on the compactability of mixtures.

2.1.1 Evaluation of Compactability

Many research efforts were performed to understand the compaction process. As part of these research efforts, different indices were proposed to interpret the compaction curves obtained from the Superpave Gyratory Compactor (SGC). The first was the slope of the compaction curve in the semi-logarithmic plot, as a result of the linear relationship between density and the logarithm of the gyrations number found by (Moutier 1974). This index is widely used as an indicator of the overall compactability.

Another proposed index is the "locking point". A closer look at the compaction curve in the semi-logarithmic plot shows that it is not entirely linear. Rather, it begins to level off at a certain number of gyrations. This number is defined as the locking point, which has the physical meaning of aggregates locking together, at which point further compaction of the mixture becomes very hard (Vavrik and Carpenter 1998). Slightly different definitions of locking point have been proposed (Vavrik and Carpenter 1998, Pine 1997, Shamsi and Mohammad 2010), but they all share the same physical interpretation: compaction becomes limited when aggregates begin locking together.

In the Superpave mix design (AASHTO R35 2015), the shape of the compaction curve is controlled by three critical gyration numbers ($N_{initial}$, N_{design}, and N_{max}). These gyration numbers were originally proposed to relate laboratory compaction effort to traffic volume and not to evaluate compactability. However, a number of researchers understood the importance of mixture compactability and started to investigate it. In one of the first studies, the authors proposed a new device, called Gyratory Load Plate Assembly (GLPA) (Guler et al. 2000), to monitor the shear resistance during compaction. Based on this work, the authors proposed an index based on energy calculated as the area under a part of the compaction curve (Guler et al. 2000). The energy index was shown to have good correlations with the compactability and stability of mixtures (Leiva and West 2008, Anderson 2002, Dessouky 2015, Yeung et al. 2016).

2.1.2 Effect of Binder Viscosity

Binder viscosity is one of the most significant factors that affects compaction. Since it is very sensitive to temperature, viscosity of binder during construction is typically controlled by temperature. Requiring a minimum temperature for mixing and compaction to ensure a relatively low viscosity of binder during compaction is one of the most effective ways to control the compaction quality. It has been shown that inadequate compaction temperature usually results in poor compaction with excessive air voids.

Asphalt Institute (AI) presented the first recommendation of the appropriate viscosity ranges for compaction and mixing of HMA (1962), which are 140 $\pm$ 15 seconds Saybolt-Furol and 85 ± 10 seconds Saybolt-Furol for mixing and compaction respectively. Compaction and mixing temperatures are then determined to achieve the proposed viscosity range. In 1974, AI changed the viscosity measurements form the units of Saybolt-Furol to units of centistokes (cSt) (Asphalt Institute 1974). The required viscosity values for compaction and mixing are 280 ± 30 cSt and 170 ± 20 cSt respectively. For the Superpave mix design, the basic concept of equi-viscous method remained unchanged. Only the units changed from cSt to Pascal-seconds (Pa·s) and the viscosity is measured using the Rotational Viscometer. The recommended viscosity values for compaction and mixing are 0.28 ± .03 Pa·s and 0.17 ± 0.02 Pa·s respectively.

The equi-viscous method works well for unmodified binders; however, a number of issues were reported when it was used on modified binder. The equi-viscous method requires an excessively high temperature (e.g. 180°C) for modified binders (Bahia and Paye 2001, Yildirim et al. 2000). This is unacceptable since it causes excessive oxidation and increases energy costs. A temperature around 160°C was found to work well for most modified binders to have the mixture well compacted (Bahia and Paye 2001, Yildirim et al. 2000). The reason has been attributed to the shear thinning phenomenon (Bahia and Paye 2001), responsible for viscosity decreases with increase in shear rate. Thus, in order to determine the compaction temperature for modified binders, the required viscosity for compaction and mixing must be related to the shear rates at which compaction or mixing occur (Bahia et al. 2006, Shenoy 2001).

In 2000, researchers at the University of Texas (Yildirim et al. 2000) developed the high-shear-rate viscosity method (HSV). In this method, the viscosity at a high shear rate is used to determine the

compaction temperature. The shear rate of compaction was estimated at $500s^{-1}$. By using HSV, the compaction and mixing temperature for the modified binder were reduced by 10 to 30°C compared to the equi-viscous method. Later the recommended viscosity ranges for mixing and compaction at the high shear rate were centered at 0.275 and 0.550 Pa s, respectively (Yildirim et al. 2006).

In 2001 researchers at University of Wisconsin developed another method called the zero-shear rate method (ZSV) (Khatri et al. 2001). This method uses the viscosity when the shear rate is zero, which based on statistical analyses, was found to correlate best with mixture compactability. The target values of ZSV for mixing and compaction were recommended as 3.0 Pa s and 6.0 Pa s, respectively. The result showed that the compaction temperature was, on average, 40°C lower than the equi-viscous method. Researchers at Indiana verified the ZSV method by comparing this method with their empirical method (Tang and Haddock 2006).

In 2001, the research group at the University of Wisconsin simplified ZSV method to low shear rate viscosity method (LSV). Compared to ZSV, LSZ simplified the interpolation process. Rather than using the viscosity at a shear rate of zero, the viscosity at the shear rate of $0.001s^{-1}$ was used to determine the compaction and mixing temperature. It was reported that LSV is simpler but can get the same result as ZSV (Bahia and Paye 2001, Bahia et al. 2006).

2.1.3 Effect of Binder Lubrication

The binder lubricity received considerable attention as part of the research on Warm Mix Asphalt (WMA) technology. WMA improves the workability of the mixture, that cannot be explained by the reduction of viscosity, since some types of WMA increase binder viscosity (Kataware and Singh 2018, Mo et al. 2012).

Hanz and Bahia (Hanz and Bahia 2013) were among the first to suggest that the increase in binder lubricity was the reason for the improvement of compaction after adding WMA. During compaction, the distance between aggregate particles decreases. In thin films or when particles are in contact, the concept of rheology does not apply, and it becomes necessary to investigate thin film behavior through the use of tribology. For two surfaces separated by a viscous fluid, rheology governs the transmission of stress when the distance between the two surfaces is large, while tribology begins to play a more important role as the distance decreases. Different configurations have been used to obtain binder lubricity, and it was found that the friction coefficient is a function of test speed, viscosity and normal load (Canestrari et al. 2017). At a controlled viscosity and normal load, the lubrication effect of binder is a function of the sliding speed. In tribology, this relationship is expressed by the Stribeck curve, as shown in Figure 2.1 (Ingrassia et al. 2018).

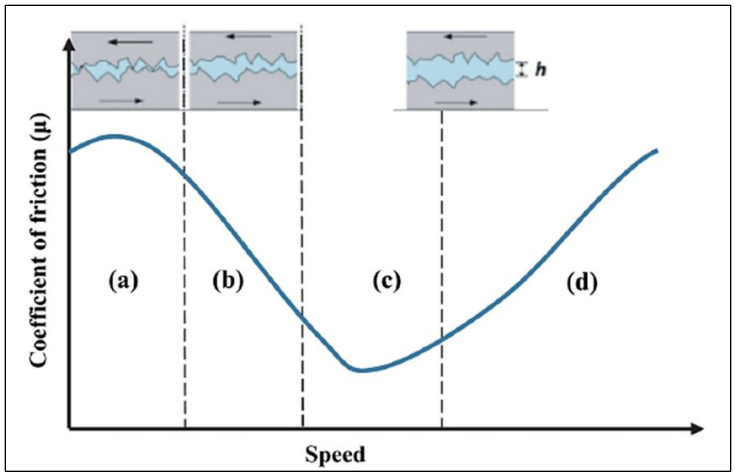

Figure 2.1 Stribeck curve: relationship between sliding speed and coefficient of friction (Ingrassia et al. 2018).

According to the Stribeck curve, the lubrication properties can be divided into four regions: "(1) the boundary regime, in which friction is mainly caused by the interaction of the asperities of the two solids; (2) the mixed regime, where a reduction of friction occurs, because the direct contact between the solids is reduced by the hydrodynamic pressure of the lubricant; (3) the elasto-hydrodynamic regime, in which the surfaces of the solids are no longer in contact and therefore the minimum friction, which is related only to the lubricant properties, is reached; (4) the hydrodynamic regime, where friction increases because of the increase in the viscous drag of the lubricant." (Ingrassia et al. 2018).

In a recent study (Yan et al. 2020) the authors performed a tribological characterization of an asphalt binder modified with graphite nanoplatelets (GNPs). Using a novel approach, in which aggregate surface microtexture was simulated using rough surfaces of the testing fixtures, it was demonstrated that the addition of GNPs lowers the friction coefficient of the asphalt binder, and therefore, enhances the lubrication properties of the binder when mixed with mineral aggregates. The outcome is a significant reduction in compaction effort to achieve target density values. The results provide a scientific explanation to previous work performed by Le et al. (2019) in which the authors found that adding a small amount of GNP significantly reduced the compaction effort for laboratory prepared asphalt mixtures as well as reheated loose mix.

2.1.4 Effect of Binder Content

In general, adding more binder helps compaction. This is the basis for the "regressing air voids" method developed in Wisconsin (West et al. 2018). However, adding more binder is more expensive and may have a negative impact on the stability of mixtures. In recent years, the use of Highly Modified Asphalt (HiMA) mixtures has received increased attention. The mixtures use a higher binder content and are compacted at much higher densities than traditional asphalt mixtures.

2.1.5 Effect of Aggregate Gradation

The effect of aggregate gradation on compaction has long been recognized. For many years, aggregates have been chosen to have gradation curves close to the maximum density line based on the 0.45 power law. However, it is not clear how the distance between the gradation curve and maximum density line affects the compactability of mixtures. In a recent investigation (Yan et al. 2022), the authors used an additional parameter called the distance to maximum density line (Dmdl), that is defined as the accumulated difference of the passing rate between the gradation curve and the maximum density line:

$$Dmdl = \sum_{\min sieve}^{\max sieve} |\%Pass\ of\ the\ sieve - \%Pass\ of\ the\ sieve\ on\ MDL\ | \quad (2.1)$$

This new parameter is derived from previous research that showed that mixture compactability is related to how close the gradation curve is to the maximum density line (Hekmatfar et al. 2015, Huber et al. 2016).

It should be noted that using a larger number of sieve sizes allows for better characterization of the aggregate gradation. In practice, however, this number is limited due to the increased cost of splitting aggregates into many sizes, and using additional aggregate bins at the hot mix plant. The aggregate gradation requirements from MnDOT specifications for construction (MnDOT 2020) are shown in Table 2.1

Table 2.1 Aggregate gradation broad bands (percent passing of total washed gradation) (MnDOT 2020)

Sieve size	A	B	C	D
1 inch	–	–	100	–
3/4 inch	–	100*	85 – 100	–
1/2 inch	100*	85 – 100	45 – 90	–
3/8 inch	85 – 100	35 – 90	–	100
No. 4	60 – 90	30 – 80	30 – 75	65 – 95
No. 8	45 – 70	25 – 65	25 – 60	45 – 80
No. 200	2.0 – 7.0	2.0 – 7.0	2.0 – 7.0	3.0 – 8.0

*The Contractor may reduce the gradation broadband for the maximum aggregate size to 97 percent passing for mixtures containing RAP, if the oversize material originates from the RAP source. Ensure the virgin material meets the requirement of 100 percent passing the maximum aggregate sieve size.

In the past decade, the Bailey method has become a popular approach for characterizing the aggregate gradation. The Bailey method was proposed by Robert D. Bailey at Illinois Department of Transportation in the early 1980s. It provided a systematic way of designing and adjusting aggregate gradation (Vavrik et al. 2002). The idea of the Bailey method is to design the interlock of the aggregates directly. A good interlocked aggregate skeleton is required for good rutting resistance. In the Bailey method, a number of parameters are used to characterize the gradation. The relationship between those parameters and the workability and volumetric of asphalt mixtures are provided, which greatly helps engineers to adjust the gradation to achieve the desired volumetric properties and compactability.

In the Bailey method, it is assumed that the coarse aggregates form the interlock and fine aggregates fill the voids of the coarse aggregates. Coarse and fine aggregates are separated by the primary control sieve (PCS), which is defined as the sieve size that equals 0.22*NMPS (normal maximum particle size). The value 0.22 was determined by 2D and 3D packing analysis of differently shaped particles. The unit weight of coarse aggregates is used to describe the degree of interlocking. Unit weight means the weight of aggregates that fills a unit volume. The loose unit weight (LUW) is the unit weight of aggregates without any compaction. This condition represents the beginning of the aggregate interlock. The rodded unit weight (RUW) is the unit weight with compaction effort applied. This condition represents the fully developed aggregate interlock. Thus, we can control the degree of interlock by choosing an appropriate unit weight. If the chosen unit weight (CUW) is 95~105% of LUW, the mixture is called coarse-graded mixture. If CUW is less than 90% of LUW, it is called fine-graded mixture. Usually, RUW equals 110% of LUW; SMA mixtures have a CUW larger than 110% of LUW. Thus, the heavier the CUW the better interlocking the mixture will be. Since the probability of degradation and the compaction effort both increase, an excessive high CUW should be avoided. CUW has a significant effect on volumetric properties. An increase in CUW over LUW will increase the air voids and VMA, while for the fine-graded mixture (CUW less than 90%), the effect of CUW on air voids and VMA is not significant.

To determine how gradation affects VMA and compactability, the gradation is separated into three portions—the coarse aggregate (sieve size larger than PCS), the coarse portion of fine aggregate (sieve size larger than SCS but smaller than PCS), and the fine portion of fine aggregate (sieve size smaller than SCS). The packing of each portion is characterized by a ratio. They are Coarse Aggregate Ratio (*CA* Ratio), Fine Aggregate Coarse Ratio (FA_c Ratio), and Fine Aggregate Fine Ratio (FA_f Ratio) respectively.

$$CA\ Ratio = \frac{(\%\ Passing\ Half\ Sieve - \%Passing\ PCS)}{(100\% - \%\ Passing\ Half\ Sieve)} \tag{2.2}$$

$$FA_c\ Ratio = \frac{\%\ Passing\ SCS}{\%\ Passing\ PCS} \tag{2.3}$$

$$FA_f\ Ratio = \frac{\%\ Passing\ TCS}{\%\ Passing\ SCS} \tag{2.4}$$

where Half Sieve is the sieve size equals 0.5*PCS. SCS is secondary control sieve which equals 0.22*PCS. Similarly, TCS is called tertiary control sieve which equals 0.22*SCS. The *CA* Ratio describes the packing characteristics of the coarse aggregate portion. Coarse particles that are smaller than the half sieve size but larger than PCS are called “interceptors”, so *CA* Ratio shows the proportion of the interceptors in the coarse aggregate portion. Interceptors are too large to fill the voids of coarse aggregates, and therefore, an increase in the *CA* Ratio will increase the difficulty of compaction and increase the air voids and VMA as well. However, if the proportion of interceptors is too low (*CA* Ratio is too low) the mixture becomes gap-graded and will be prone to segregation. The FA_c Ratio describes the packing characteristics of the coarse portion of the fine aggregate. As this ratio increases, the fine aggregates become denser and the

VMA decreases. Noticeably, this ratio typically has the most significant effect on VMA. A similar trend of effect can be seen in FA_f ratio.

In conclusion, PCSI characterizes the overall fineness of the aggregates, *CA* Ratio characterizes the fineness of coarse aggregates (aggregates larger than PCS), *FAc* characterizes the fineness of coarse portion of fine aggregates (aggregates larger than SCS but smaller than PCS), and FAf characterizes the fineness of fine portion of fine aggregates (aggregates smaller than SCS). The influence of CUW, *CA* Ratio, FA_c Ratio, and FA_f Ratio on VMA and workability is summarized in Table 2.2.

Table 2.2 Summary of the Bailey method

Bailey Method Indices	VMA	Workability
CUW: Chosen Unit Weight	5% increase in unit weight will increase VMA by 0.5 to 1.0%. For fine-graded mixtures, the effect is not significant.	An increase in CUW will decrease compactability
CA Ratio: Coarse Aggregate Ratio	An increase of 0.2 in the *CA* Ratio will result in an increase of 0.5 to 1.0% VMA.	A decrease in *CA* Ratio will increase compactability, but also segregation.
FA_c Ratio: Fine Aggregate Coarse Ratio	A decrease of 0.05 in the FA_c Ratio will create an increase of 0.5 to 1.0% in VMA.	An increase of FA_c Ratio will increase compactability.
FA_f Ratio: Fine Aggregate Fine Ratio	A decrease of 0.05 in the FA_f Ratio will create an increase of 0.5 to 1.0% in VMA.	An increase of FA_f Ratio will increase compactability.

In a recent publication (Yan et al. 2023), used binary aggregate packing concepts to modify four traditional Superpave asphalt mixtures, used in Minnesota projects, into high-compactability mixtures. The authors showed that the proposed method provides a theoretical explanation for the maximum density line (MDL) and the Bailey method, and revealed their limitations. The experimental results showed that, due to their denser aggregate packing, the high-compactability mixtures outperform the traditional Superpave mixtures. The authors proposed high-compactability mix design framework that provides a rational and practical approach to improve the field density and the overall quality of asphalt pavements.

2.1.6 Effect of Other Properties of Aggregates

In the experimental study of Leiva and West (2008), aggregate-related properties such as type, shape, and nominal maximum aggregate size (NMAS) were studied. It was found that fine-graded mixtures are more compactable than coarse-graded mixtures; SMA were the most difficult to compact. In terms of NMAS, it was found that compactability of the mixture decreases with increasing NMAS. The same trend had been also observed by Gudimettla et al. (2003).

In terms of aggregates type, it was found that mixtures containing limestone as the primary aggregate source tended to be difficult to compact. The main differences between limestone and other aggregate types are that they are tougher, more angular and contain more mineral filler. Marble-schist mixtures are more easily compacted, followed by granite mixtures. Marble-schist aggregate is characterized by

flat and elongated particles and low strength aggregates. These properties are related to aggregate degradation and allow denser aggregate packing to be achieved. On the other hand, granite mixtures contain some flat and elongated particles and intermediate aggregate strength, but most of these mixtures are fine graded, which may explain their ability to be easily compacted. In general, the marble-schist and granite mixtures were easier to compact than the limestone mixes.

Mineral filler is composed of particles passing the No. 200 sieve (<0.075mm). It is so small that it is usually considered as part of binder suspension (mastic) and it is not included in the aggregate gradation. The mineral filler was found to improve the rutting resistance of the mixture (Kallas et al. 1962, Wang et al. 2011) but it increases the compaction efforts as well (Kallas et al. 1962) If the mineral filler and binder are considered together as the mastic, it is shown that the dosage of mineral filler increases the viscosity of mastic (Hesami et al. 2012), which is probably the main reason for which mineral filler increases the compaction efforts.

Gudimettla et al. (2003) studied the shape of aggregates. The authors showed that mixtures prepared with cubical, angular granite were less workable than mixes prepared with semi-angular crushed gravel. It was found that elongated and flat aggregates are more difficult to compact, compared with round aggregates.

The effect of fine aggregate angularity (FAA) on compaction was studied by Stakston et al. (2002). For laboratory compaction below 92% Gmm (representative of construction compaction), a consistent trend of higher resistance to compaction with higher FAA was observed. For compaction above 92% Gmm, the effect of FAA on compaction is inconsistent and is dependent on the source of aggregate and gradation.

In MnDOT current specification (MnDOT 2018), the aggregate angularity is quantified by the Coarse Aggregate Angularity (CAA) of one face and two faces (ASTM D5821), and the Fine Aggregate Angularity (FAA) (AASHTO T304 Method A). The aggregate properties requirements of MnDOT specification (MnDOT 2018) are shown in Table 2.3. It can be seen that angularity increases with the increase in traffic level. For RAP materials, the combined RAP and virgin aggregates need to meet the composite coarse and fine aggregate angularity for the mixture being produced.

Table 2.3 Aggregate gradation requirement specified by MnDOT (MnDOT 2018)

Aggregate Blend Property	Traffic Level 2	Traffic Level 3	Traffic Level 4	Traffic Level 5
20 year Design ESAL's	< 1 million	1 – 3 million	3 – 10 million	10 – 30 million
Min. Coarse Aggregate Angularity (ASTM D5821)				
(one face / two face), % - Wear	30 / -	55 / -	85 / 80	95 / 90
(one face / two face), % - Non-wear	30 / -	55 / -	60 / -	80 / 75
Min. Fine Aggregate Angularity (FAA) (AASHTO T304, Method A)				
% - Wear	40	42	44	45

Aggregate Blend Property	Traffic Level 2	Traffic Level 3	Traffic Level 4	Traffic Level 5
%-Non-wear	40	40	40	40
Flat and Elongated Particles, max % by weight	-	10 (5:1 ratio)	10 (5:1 ratio)	10 (5:1 ratio)
Min. Sand Equivalent (AASHTO T 176)	-	-	45	45
Max. Total Spall in fraction retained on the #4 sieve				
Wear	5.0	2.5	1.0	1.0
Non-wear	5.0	5.0	2.5	2.5
Maximum Spall Content in Total Sample				
Wear	5.0	5.0	1.0	1.0
Non-wear	5.0	5.0	2.5	2.5
Maximum Percent Lumps in fraction retained on the #4 sieve	0.5	0.5	0.5	0.5
Class B Carbonate Restrictions				
Maximum % -#4				
Final lift/All other lifts	100 / 100	100 / 100	80 / 80	50 / 80
Maximum % +#4				
Final lift/All other lifts	100 / 100	100 / 100	50 / 100	00 / 100
Max. allowable scrap shingles-NWSS wear/non wear	5 / 5	5 / 5	5 / 5	5 / 5
Max. allowable scarp shingles-TOSS final lift/all other lifts	5 / 5	5 / 5	0 / 5	0 / 0

*NWSS is manufactured waste scrap shingle and TOSS is tear-off scrap shingle.

2.2 Compaction of RAP Mixtures

As already mentioned, the use of Reclaimed Asphalt Pavement (RAP) has significantly increased over the years due to considerable economic benefits and reduction in environmental impact. However, unlike the traditional components of asphalt mixtures, the aggregates and the asphalt binder, there is less control of the properties of the RAP material used, which includes RAP source, size and gradation of RAP particles, aged binder grade and available binder content. All of these factors can significantly affect the compaction characteristics, performance, and durability of asphalt mixtures, especially when higher percentages of RAP are used in the mix design.

Most of these factors are addressed in two comprehensive reports from FHWA and NAPA, respectively (Copeland 2011, Newcomb et al. 2016). Both reports provide guidelines for RAP processing and stockpile management, and discuss in detail receiving and storage of materials, stockpile blending prior to crushing, sizing, RAP storage, and characterization of the produced RAP. Variability of RAP properties

can be high, unless stockpile blending is utilized prior to crushing and sizing, which is critical if the stockpiles contain materials that are significantly different from one another. Well separated stockpiles can save time and cost for crushing or fractionating RAP. However, crushing to a smaller maximum size can increase the amount fine materials in the RAP and limit the amount of RAP that can be incorporated into a recycled mixture. Fractionating RAP is also discussed, as a viable method to better control gradation. Generally, RAP is fractionated into two (coarse and fine aggregate) or three sizes (oversize, coarse and fine aggregates). Moisture in RAP and virgin aggregate is undesirable, and guidelines are provided on how to reduce it. To consider the stiffening effect of the aged binder in RAP, the specified binder grade has to be adjusted. For RAP content lower than 15%, no change in binder selection is required, for 15-25% RAP content, virgin binder is selected with one grade softer, and for more than 25% RAP content, a blending chart is used, with the assumption of complete blending between virgin and RAP binder. In many cases, RAP content is specified according to the percentage of binder replacement. Solvent extraction and ignition oven are discussed as methods used to determine the asphalt content of RAP.

In a review on the challenges of using higher amounts of RAP for new asphalt mixtures (Tarsi et al. 2020), the authors identify the key barriers to increasing RAP use, and provided guidelines on how to overcome these barriers. The authors focused on issues related to the quality and homogeneity of RAP materials, current plant production technologies, mix design methods, evaluation of the degree of blending and diffusion that occurs between the virgin and aged binders, and the use of rejuvenators, and performance of asphalt mixtures containing RAP.

One method that provides a better control of the size of RAP particles is using fractionated RAP. In a previous research effort performed by MnDOT, Johnson et al. (2012) investigated the potential benefits of using fractionated RAP for three test sections at the Minnesota Road Research Facility (MnROAD). All three sections contained 30 percent RAP, but vary by binder grade and fractionated RAP content. Both fractionated and non-fractionated RAP stockpiles consisted of bituminous mixture material removed from the MnROAD test facility. The coarse portion of the fractionated RAP was obtained as the portion of the RAP retained on the No. 4 sieve. The fine portion of the fractionated RAP had 100 percent passing the No. 4 sieve.

The asphalt mixtures used in cell 20 had 30 percent non-fractionated RAP by weight of total aggregate, for both SPWEB440B wearing course and SPNWB440B non-wearing course. Cell 21 incorporated 30 percent fractionated RAP by weight of total aggregate, for both SPWEB440B Special wearing course and SPNWB440B Special non-wearing course mixtures. The proportions of coarse and fine RAP fractions were determined from mixture design recommendations. Cell 22 incorporate 30 percent fractionated RAP by weight of total aggregate, for both SPWEB440C Special 1 wearing course and the SPNWB440C Special 1 non-wearing course mixtures. The proportions of coarse and fine RAP fractions were again determined from mixture design recommendations. The approved mixture designs included the following components:

- 30 percent MnROAD millings
- Non-fractionated mixture includes approximately 24 percent fine plus 6 percent coarse (Cell 20)

- Fractionated mixture includes 20 percent fine plus 10 percent coarse (Cells 21 and 22)
- 35 percent washed manufactured sand
- 20 percent 0.5-in. chips
- 15 percent unwashed 0.75-in. rock

The final designs of each cell used identical percentages of RAP and aggregate material for the wear and non-wear mixtures. The asphalt cement content of the non-fractionated mixture increased 0.3 percent between wear and non-wear designs, and the asphalt content increased 0.2 percent between mixtures for the fractionated designs. At the end of a four-year analysis of pavement performance, after construction, no significant differences were observed among the three test sections.

A different outcome was observed by Stimili et al. (2015a, 2015b) in an investigation on the performance of hot recycled mixtures containing SBS modified binder. The authors performed a laboratory study on the assessment of the mechanical properties of hot recycled mixtures prepared with high percentage of RAP including aged SBS modified binder. A comparison, between the reference mixture (REF) with 25% RAP and four mixtures containing 40% of fractionated RAP, was conducted. The mixtures with 40% RAP were designed using the Bailey method, based on previous work by Graziani et al. (2012). Two polymer modified bitumen were used as virgin binder: Soft (S) and Hard (H) characterized 1.8% and 3.8%, respectively, by the binder weight of Styrene-Butadiene-Styrene (SBS) polymer. Two binder contents, 5% and 5.2% by aggregate weight, were used in the design.

Three fractions of virgin crushed limestone aggregates (10/20mm, 4/10mm, 0/4mm) were selected to produce all five mixtures. For the reference mixture, 25% of RAP 0/16mm was used, while for the 40% RAP mixtures, RAP was divided into two fractions: 0/8mm and 8/16mm. The binder content of RAP was determined to be 4.9%, while for the RAP fraction 0/8mm was 6.4% and for the RAP fraction 8/16 was 5.0% of aggregate weight.

The reference mixture was prepared with (H) as virgin binder. All four mixtures containing 40% RAP were characterized by the same grading curve that was designed using Bailey method to achieve an optimized aggregate packing. All mixtures were compacted at 160°C using a Superpave Gyratory Compactor, to obtain cylindrical specimens having diameter (D) = 150 mm and height (H) = 170 mm, and a target air void content of 3.5%,

To evaluate the compatibility properties of the mixtures, the authors used the Compaction Energy Index (CEI), which represents the area under the compaction curve. A higher CEI value indicates a less compactable mixture. The increase in RAP content would cause a reduction in the mixture compactability, due to higher amount of stiff binder and higher RAP variability, and the authors wanted to evaluate if using Bailey method, and RAP fractioning, to optimize aggregate gradation, would offset this negative effect of higher RAP content. The compactability assessment was supplemented with image analysis of internal aggregate structure to evaluate aggregate packing. The analysis was performed on 2-dimensional images of mixture section processes through specific software (Sefidmazgi et al. 2012) that allow the calculation of two internal structure parameters: the total aggregate proximity zone length and the aggregate-on-aggregate number of contact points. The higher the

proximity zone length and the number of contact points, the stronger the interlocking between aggregates.

The results showed that the highest CEI value was obtained for the control mixture. Lower compaction energy was observed for all mixture with 40% RAP. The lowest values were found for the mixtures prepared with less modified bitumen (1.8% SBS). The findings were also confirmed by the image analysis results, in terms of proximity zone length and number of contact points. In addition, the authors found that the low temperature performance was better for the mixtures with 40% RAP. In particular, the mixtures that contained more modified virgin bitumen (3.8% SBS). Although limited, the results suggested that a proper selection and processing of RAP materials (fractioned in two sizes, coarse and fine) as well as a more refined mix design (Bailey Method) can overcome the stiffening effect caused by an increase of 15% of RAP.

A similar approach, based on Bailey method, was followed in a more recent publication from the same research group, to investigate the performance of dense-graded warm mixtures with reclaimed asphalt (D'Angelo et al. 2024). In this case, three warm mix asphalt mixtures (WMA), were compared to a reference mixture. A dense graded HMA containing 30% RA and 4.3% SBS was taken as the reference mixture. The WMA were produced using different asphalt contents of polymer modified bitumen (4% SBS): 4.4% (A), 4.6% (B) and 4.8% (C). In addition, an amino-type chemical additive, specific for WMA technology and with adhesion activator qualities, was used for the production at lower temperature. The dosage was 0.60% by weight of virgin bitumen. The design gradation curves were optimized in terms of volumetric characteristics by applying Bailey Method. A mixing temperature of 130°, which is 40°C lower than the reference mixture temperature, was used to produce both laboratory and in-plant WMAs.

The workability of the mixtures was evaluated by calculating the Compaction Energy Index (CEI) from the gyratory data. For dense-graded mixture, the CEI is calculated as the area under the compaction curve starting from the 8^{th} gyration up to a compaction level equal to 92% of the mixture maximum density G_{max}. The results, presented in Figure 2.2, in terms of average CEI and residual AV content calculated at 200 revolutions, show that in spite of the lower production temperature and increased RA content, as compared to the reference mix, the WMA mixtures had acceptable values CEI. However, it should be noted that the increase in total bitumen content (mixture C) improves the compactability of WMA mixture, even though too low residual AV are expected.

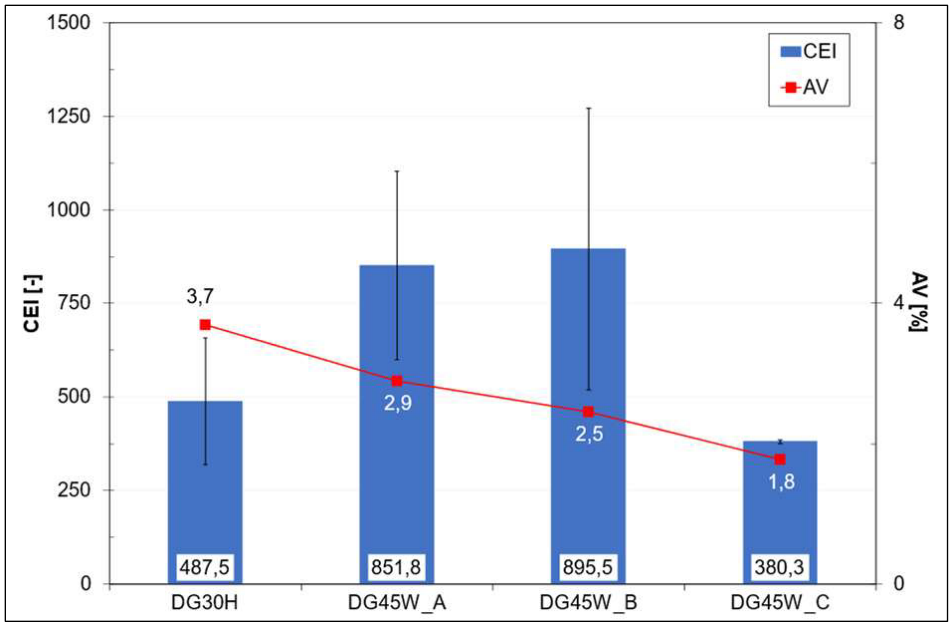

Figure 2.2 CEI and air voids (AV) for all WMA and the reference mixtures (D'Angelo et al. 2024).

From further laboratory experimental work, the authors found out that the increase in RAP content did not negatively affect the mechanical performance, in terms of strength properties, cracking propensity and water sensitivity of warm mixture as compared to the reference HMA, validating the effectiveness of the WMA technology in mitigating the potential aging effects of high RAP content. However, an excessive stiffness, attributable to the higher amount of RAP but also to lower residual AV content can result in WMA mixture more prone to fatigue failure.

To better characterize the outcome of crushing and screening of RAP, Zaumanis et al. (2022) proposed three new indices: chunk index, breakdown index, and filler increase (CBF indices). The indices are derived from the black and white grading curves of RAP, which have been used for sieves analysis of mixtures with RAP. The black curves represent the gradation of RAP particles from fractioned RAP, and the white curves are the gradation of recovered RAP aggregate after binder e RAP will hold chunks of many individual pieces.

A RAP piece can be only one particle coated with a thin binder film, or it can consist of a combination of large and small particles, or many small particles. The size of these "chunks" can vary greatly depending on the method of producing RAP. For example, when milling a pavement, the size of the chunks depends on the type of the milling machine, the depth of milling, the moving speed of the machine, toughness of the aggregates, the rotation frequency of the drum, the pavement type, its age, and even the environmental conditions. The Chunk index represents the difference between RAP chunks and a theoretical scenario when all the RAP particles are separated. It is calculated as the difference between the area below the processed white and processed black curves, see Figure 2.3.

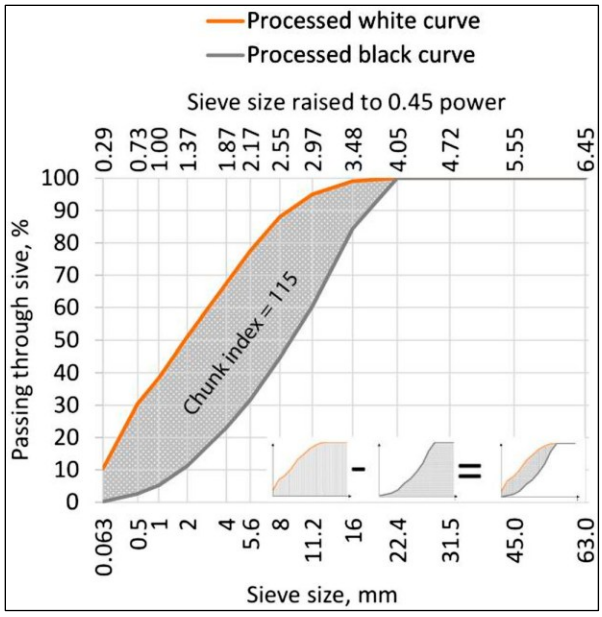

Figure 2.3 Chuck Index example (Zaumanis et al. 2022).

In many cases, a reduction of RAP aggregate particle size is not desirable, since it can limit the maximum amount of RAP that can be added. The lack of coarser aggregates in RAP is especially detrimental when it is intended for the production of base and binder course mixtures, for which significantly higher RAP content is allowed. The Breakdown index represents how much finer the RAP aggregates have become as a result of RAP processing, and it is calculated as the difference between the area below the processed white and source white curves. An example is shown in Figure 2.4.

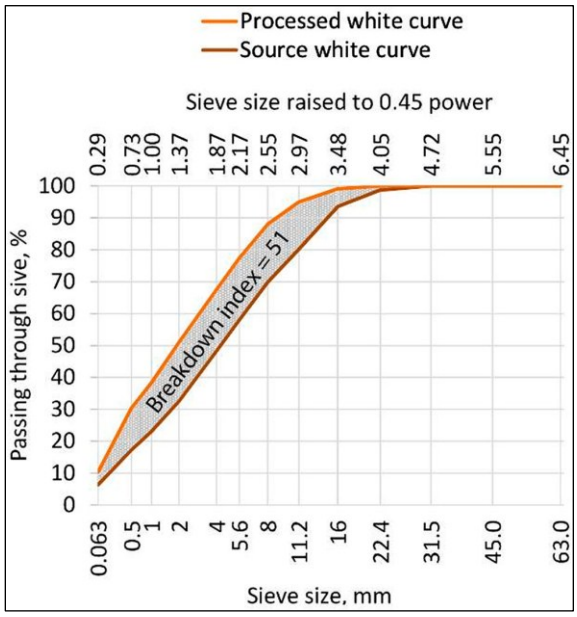

Figure 2.4 Example of Breakdown Index (Zaumanis et al. 2022).

For situations when the aggregate size is too large and the available RAP needs to be further crushed to a single size, this index should not be used in the evaluation of RAP processing.

As a result of milling and processing, the filler (material below 0.063 mm) content of RAP can be as high as 10% to 20%. Such an excessive filler will negatively affect the volumetric and grading curve requirements of the asphalt mixtures. In many cases, the excessive filler content and not the aged binder sets the limits for how much RAP can be added to the mixtures. While using rejuvenators can compensate for the aged binder effect, the only method to reduce the filler content of RAP is to reduce the amount of the RAP fraction that contains the filler. The increase of filler content is already a part of the Breakdown index. However, to better highlight the increase in filler content, the authors proposed using a separate index, the Filler increase index, that is calculated as the difference between the filler content of the processed white curve and the source white curve. An example is shown in Figure 2.5.

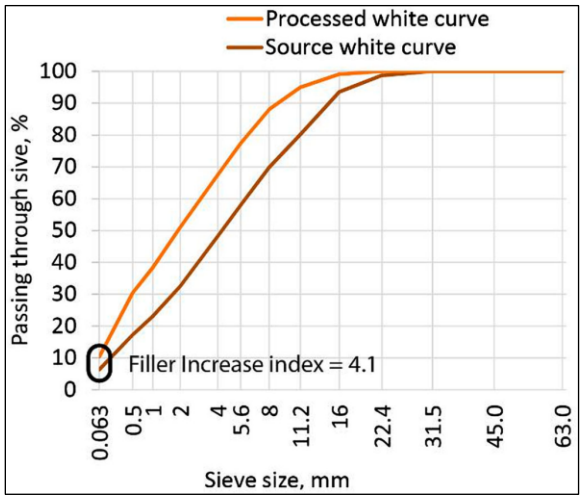

Figure 2.5 Filler increase index (Zaumanis et al. 2022).

It was proposed to use all three CBF indices to evaluate different processes and materials. An example is shown in Figure 2.6.

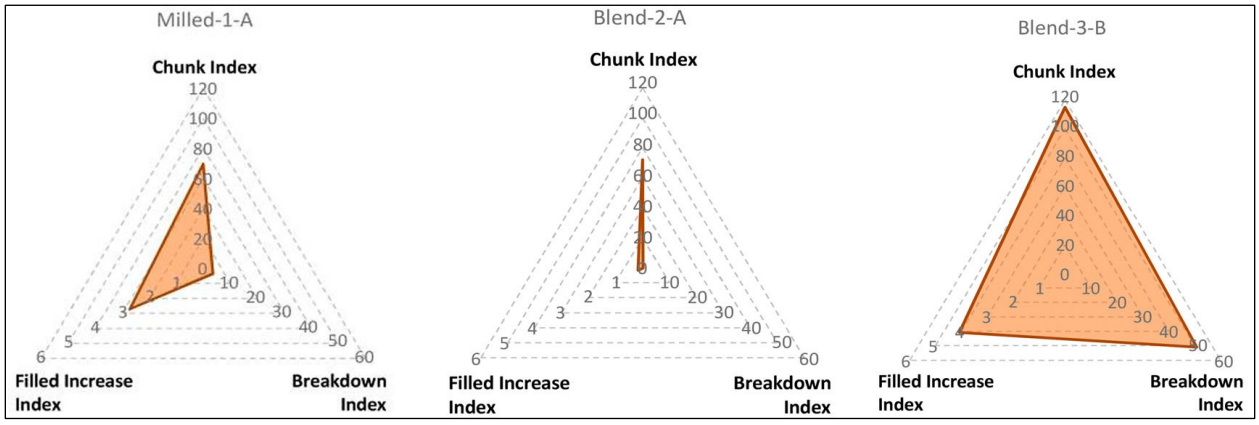

Figure 2.6 Radar chart for comparing different RAP processing setups (Zaumanis et al. 2022).

Chapter 3: Experimental Investigation on Compaction Performance of RAP Materials

The research team collected various sources of RAP and performed gyratory compaction experiments under various RAP contents. Based on a developed mixture design spreadsheet, the research team investigated how RAP content affected optimum gradation curve for compaction performance. This chapter presents this experimental investigation.

3.1 Raw RAP Material

The research team collected three sources of RAP material for preliminary characterization: Bituminous Roadways BR-Millings and BR-RAP, and MnROAD Cell 78 millings. The MnROAD Cell 78 mixture was a SPWEB340C, designed for wearing course and aggregate size of 3/4 inch. It was designed for 1 to 3 million ESALs traffic and had a design air void of 4%. The asphalt binder used was a PG 58-34. At 60 design gyrations, the mixture had a density of 147.7 lbs./ft^3. The three RAP sources are shown in Figure 3.1.

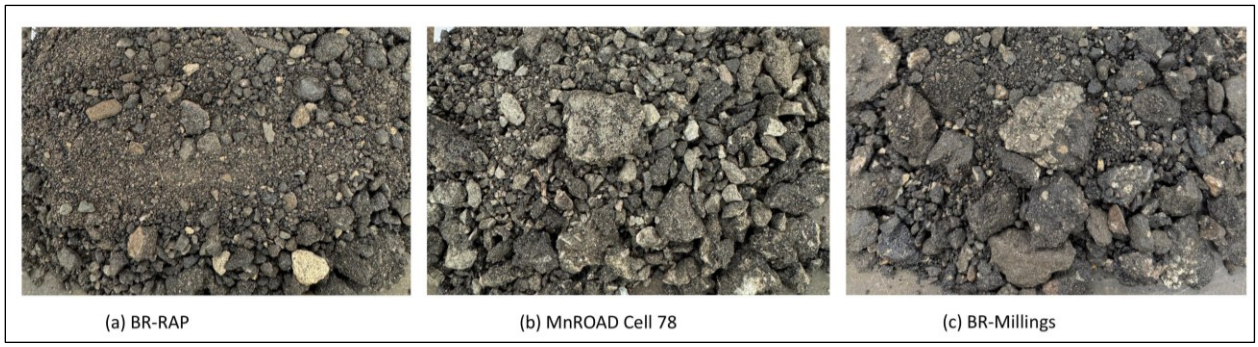

Figure 3.1 Raw RAP materials collected for the experimental investigation.

3.2 Processed White and Black Curves

Zaumanis et al. (2021) discussed the concepts of processed black curve, processed white curve, and the chunk index, that represent useful tools to characterize RAP materials. The processed black curve refers to the gradation of fractioned RAP including binder. The gradation of fractioned RAP, without the binder, is referred to as the processed white curve. In an ideal case, where all RAP particles are fully separated, the processed black curve and processed white curve would overlap since the bitumen would be uniformly exposed to heat and blend properly with the new mix. The chunk index represents the difference between RAP particles (chunks) and a theoretical scenario when all the RAP materials are separated:

$$\text{Chunk index} = A_{\text{PW}} - A_{\text{PB}} \tag{3.1}$$

where A_{PW} = The area below the processed white curve, where the sieve size is raised to 0.45 power, and A_{PB}= The area below the processed black curve, where the sieve size is raised to 0.45 power.

A smaller chunk index indicates that the processed white and black curves are closer together, which indicates that fewer individual aggregate particles are stuck together in agglomerations, and for asphalt production smaller chunk is the first objective of RAP processing because it indicates a homogenous asphalt mixture. By contrast, a higher chunk index means that more RAP aggregates are held together in chunks, which results in a poor interaction between RAP and virgin materials, and leading to inhomogeneous mixture composition (Zaumanis and Mallick 2013, Ding et al. 2016, Sreeram et al. 2018, Zaumanis and Haritonovs 2018, Lo Presti et al. 2019). The processed black curve, processed white curve, and the chunk index are illustrated in Figure 3.2, where the chunk index is shaded in grey color.

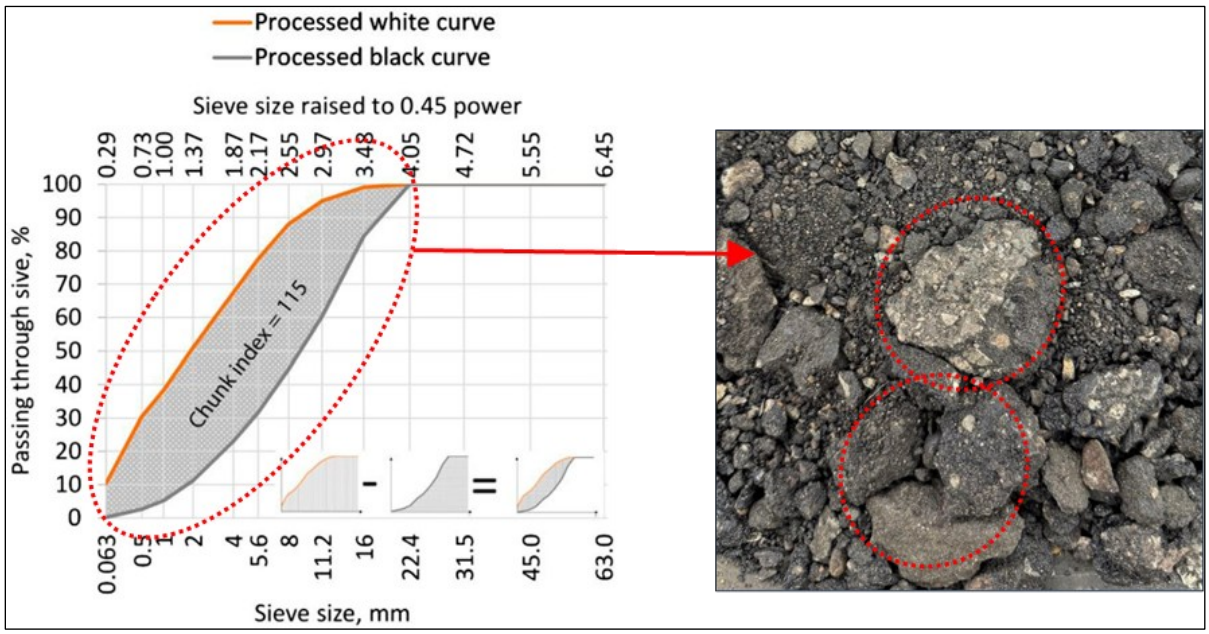

Figure 3.2 Chuck index plot.

The research team considered BR-RAP, BR-Milling and MnROAD Cell 78 to be fractionated RAP material. The binder content of each RAP material was calculated by ignition oven test. The gradation of RAP material before and after ignition oven was considered as the processed black curve and processed white curve, respectively. To calculate the binder content, we first determine the difference in the weights of RAP after heating at 110 ℃ and after the ignition oven. The binder content is then calculated as the ratio between this weight different and the weight of the RAP after heating at 110 ℃, i.e.:

$$\text{Binder Content} = \left(\frac{X - Y}{X}\right) \times 100\% \tag{3.2}$$

where, X= Weight of the RAP after heating at 110 ℃, gm and Y= Weight of the RAP after Ignition oven, gm. The moisture content of RAP was determined by weight difference before and after heating the RAP to 110℃, while the binder content of RAP was calculated by ignition oven test using Equation 3.2. Table

3.1 shows the moisture content and binder content of RAP material. BR-RAP, BR-Milling, and MnROAD Cell 78 Milling were sieved following the ASTM C136 (2006). Aggregate gradation is shown in Table 3.2

Table 3.1 Moisture and asphalt contents of RAP materials

RAP Source	Moisture Content (gm)	Binder Content %
BR-RAP	14.3	5.66
BR-Milling	18.2	7.094
MnROAD Cell 78	7.1	5.25

Table 3.2 Gradation of BR-RAP, BR-Milling, and MnROAD Cell 78 Milling

Sieve size	Percent Passing (%)					
	Processed Black Curve			Processed White Curve		
	BR-RAP	BR-Milling	MnROAD Cell 78 Milling	BR-RAP	BR-Milling	MnROAD Cell 78 Milling
1 in, 25mm	97.1	100	100	100	100	100
3/4 in, 19mm	96.7	97.8	88.9	100.0	100	88.4
1/2 in, 12.5mm	90.2	85.5	70.0	98.3	92.7	71.9
3/8 in, 9.5 mm	80.6	70.6	59.3	93.4	71.1	64.7
No.4, 4.75 mm	55.6	43.1	31.9	73.6	56.5	47.4
No.8, 2.36 mm	38.6	25.7	15.4	57.3	42.7	34.6
No.16, 1.18mm	25.5	14.1	6.1	44.9	22.1	25.3
No.30, 0.6mm	11.8	9.0	2.1	31.7	9.5	18.7
No.50, 0.3mm	1.2	2.5	0.1	15.9	4.1	13.7
No.100, 0.15mm	0.0	0.0	0.0	6.2	1.6	10.0
No.200, 0.075 mm	0.0	0.0	0.0	2.7	0.0	7.3

Figure 3.3 represents the gradation curves for different RAP materials. The process black curves represent gradation with RAP chunks intact, and the white curves represent the gradation of the aggregates after the binder was extracted from RAP, and the chunks have been broken down. The processed black curve is named as Black Curve BR-RAP, Black Curve BR-Milling, and Black Curve MnROAD Cell 78, while the processed white curve White Curve BR-RAP is named as White Curve BR-Milling, and White Curve MnROAD Cell 78. It is observed that, for the black curves, there is a distinct gradation difference between the three different types of RAP material, whereas the white curves of MnROAD Cell 78, and BR-RAP have nearly identical gradations. This signifies that removing the binder from the RAP material results in identical gradations of the different sources of RAP materials.

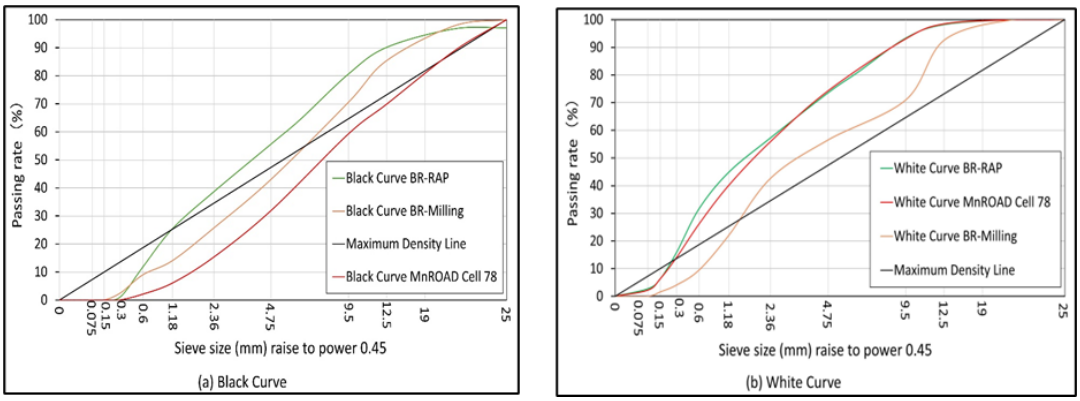

Figure 3.3 Gradation of RAP materials of BR-Milling, MnROAD Cell 78, and BR-RAP.

Figure 3.4 represents the difference of the area under the processes white curve and processes black curve. The MnROAD Cell 78 has high chunk index value of 101.28, compared to BR-Milling, and BR-RAP, meaning the MnROAD Cell 78 has large amount of RAP chunks. As can be seen from Figure 3.3 (a) and (b) the Black Curve MnROAD was much coarser while the White Curve MnROAD became significantly finer. The high chunk index suggests that proper RAP processing is necessary to achieve finer gradation suitable for mixing with virgin materials. The Chunk Index of BR-Milling is the lowest 22.4 amongst the three-chunk index (Figure 3.4 (b)), which indicates that the processed black and white curves are much closer. This signifies that fewer individual aggregate particles remain bound in the agglomeration, making BR-Milling the most suitable RAP material for mix design.

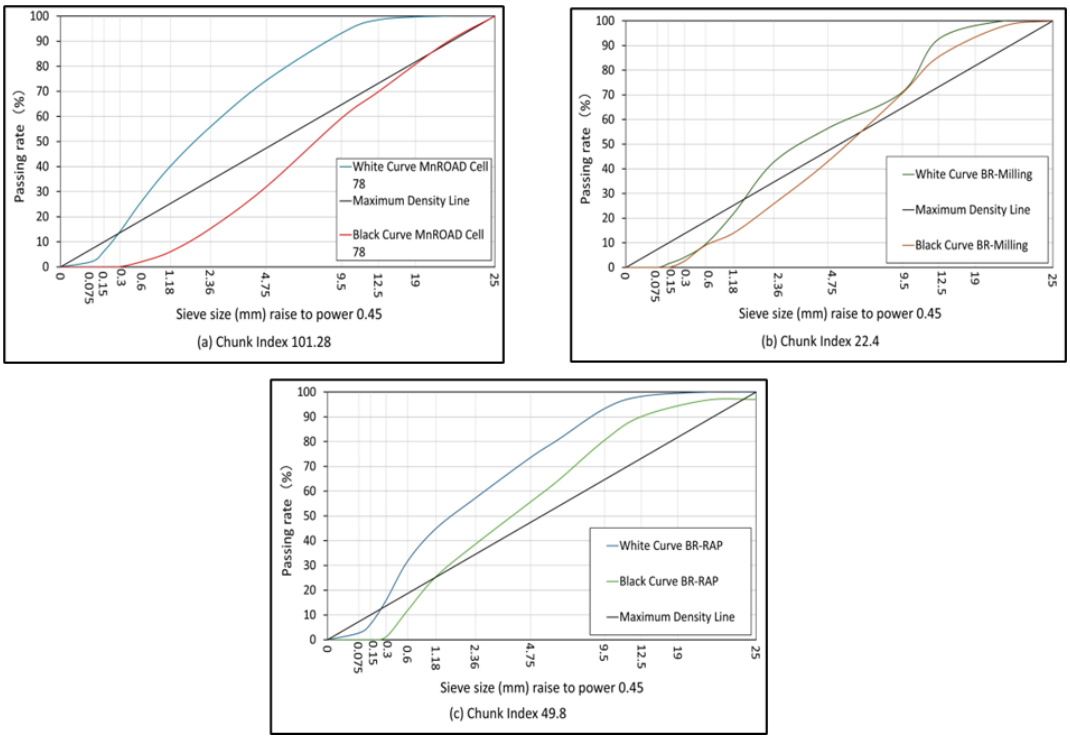

Figure 3.4 Chuck indices of BR-Milling, MnROAD Cell 78, and BR-RAP.

3.3 Materials and Method of Mix Design

3.3.1 Materials

The raw materials from three projects using Superpave 5 mixture were collected in fall of last year. The three mixtures were identified as Mix 1 (TH 30), Mix 2 (South TH4), and Mix 3 (North TH4). The research team labelled the RAP from Mix 1 as RAP A, from Mix 2 RAP B, and from Mix 3 as RAP C. All three mixtures were used in the wearing course. In the mix design report for Mix 1, it was mentioned that RAP A was fractioned, whereas no such information was provided for RAP B of Mix 2 or RAP C of Mix 2. The three RAP materials are shown in Figure 3.5. It can be seen that both RAP B and RAP C contain larger chunks of RAP that would require mechanical crushing prior to using them in mixture preparation. For this reason, only Mix 1 and the corresponding RAP A was used to prepare mixtures with different percentages of RAP for evaluating the compaction properties.

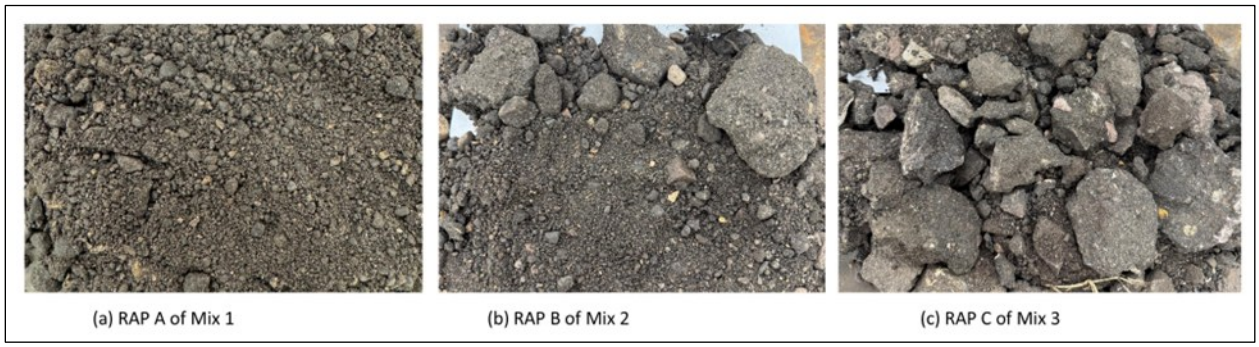

Figure 3.5 RAP material collected for Superpave 5 projects.

The volumetric properties of Mix 1, Mix 2, and Mix 3, provided by the asphalt mix design contractor, are presented in Table 3.3 to Table 3.8. Mix 1, labeled as 2360-SPWEB350, was designed for wearing course and has nominal maximum aggregate size of 3/4 inch. It is designed for 1 to 3 million ESALs and has a design air void 5%. The asphalt binder used was a PG 58S-28. At 30 design gyrations, the mixture density is 145.9 lbs./ft^3. Mix 2, labeled as SPWEB450F, is designed for wearing course and has nominal maximum aggregate size of 3/4 in. It is designed for 3 to 10 million ESALs traffic and has a design air void for 5%. The asphalt binder used was a PG 58V-34. Mix 3, labeled as 2360-SPWEB450, is designed for wearing course and has nominal maximum aggregate size of 3/4 in. It is designed for 3 to 10 million ESALs traffic and has a design air void for 5%. The asphalt binder used was a PG 58V-34. At 50 design gyrations, the mixture has a gyratory density of 144.9 lbs./ft^3.

Table 3.3 Composite gradation of Mix 1

Sieve Size	% Passing	Specification
1 Inch, 25 mm	100	100
3/4 Inch, 19 mm	100	97-100
1/2 Inch, 12.5 mm	93	85-100
3/8 Inch, 9.5 mm	86	35-90

Sieve Size	% Passing	Specification
No.4, 4.75 mm	64	30-80
No.8, 2.36 mm	47	25-65
No.16, 1.18 mm	34	
No.30, 0.6 mm	25	
No.50, 0.3 mm	15	
No.100, 0.15 mm	7	
No.200, 0.075mm	4.1	2.0-7.0

Table 3.4 Volumetric properties of Mix 1.

Parameter	Mix Design	Specification
% Iso Voids	5.0	4.0-6.0
% Total AC	5.8	5.4
% New AC	4.6	
% New/% Total AC	79.3	70
Surface Area	26.6	
% VMA	16.1	
Use of Anti-Strip Required:	No	
Contains RAP:	Yes	
Contains RAS:	No	

Table 3.5 Composite gradation of Mix 2.

Sieve Size	% Passing	Specification
1 Inch, 25 mm	100	100
3/4 Inch, 19 mm	100	97-100
1/2 Inch, 12.5 mm	96	85-100
3/8 Inch, 9.5 mm	86	35-90
No.4, 4.75 mm	59	30-80
No.8, 2.36 mm	50	25-65
No.16, 1.18 mm	39	
No.30, 0.6 mm	28	
No.50, 0.3 mm	17	
No.100, 0.15 mm	8	
No.200, 0.075mm	4.4	2.0-7.0

Table 3.6 Volumetric properties of Mix 2.

Parameter	Mix Design	Specification
% Total AC	5.6	
% New AC	4.5	
% New/% Total AC	80.9	80
% Absorbed Asphalt	0.40	
% Effective Asphalt	5.22	
Dust/Effective Asphalt	0.85	0.6-1.2
RAP Fine Aggregate Angularity	42.0	
Contains RAP:	Yes	

Table 3.7 Composite gradation of Mix 3.

Sieve Size	% Passing	Specification
1 Inch, 25 mm	100	100
3/4 Inch, 19 mm	99	97-100
1/2 Inch, 12.5 mm	87	85-100
3/8 Inch, 9.5 mm	79	35-90
No.4, 4.75 mm	65	30-80
No.8, 2.36 mm	49	25-65
No.16, 1.18 mm	35	
No.30, 0.6 mm	24	
No.50, 0.3 mm	14	
No.100, 0.15 mm	7	
No.200, 0.075mm	4.8	2.0-7.0

Table 3.8 Volumetric properties of Mix 3.

Parameter	Mix Design	Specification
% Iso Voids	5.0	4.0-6.0
% Total AC	5.6	5.4
% New AC	4.6	
% New/% Total AC	82.1	70
Surface Area	27.5	
% VMA	15.7	
Use of Anti-Strip Required:	No	
Contains RAP:	Yes	
Contains RAS:	No	

3.3.2 Laboratory Characterization of RAP Materials

For RAP A of Mix 1 three replicate tests were performed. The gradation was determined according to ASTM C136 standard (ASTM 2006), and the results are shown in Table 3.9.

Table 3.9 Gradation of RAP A of Mix 1.

Sieve size	Passing rate (%)					
	Processed White Curve			Processed Black Curve		
	White Curve 1	White Curve 2	White Curve 3	Black Curve 1	Black Curve 2	Black Curve 3
1 in, 25mm	100.0	100.0	100.0	97.3	97.4	97.2
3/4 in, 19mm	97.9	95.7	96.3	92.9	87.1	85.8
1/2 in, 12.5mm	92.6	92.8	92.9	89.0	79.9	73.9
3/8 in, 9.5 mm	83.1	86.0	84.1	79.1	68.1	58.5
No.4, 4.75 mm	76.0	80.9	78.5	71.5	59.4	48.9
No.8, 2.36 mm	51.9	63.3	57.9	49.4	37.5	27.7
No.16, 1.18mm	38.6	47.7	43.1	33.0	24.4	17.6
No.30, 0.6mm	27.2	31.9	29.1	15.9	12.6	9.7
No.50, 0.3mm	14.4	16.4	15.0	3.1	3.4	3.3
No.100, 0.15mm	6.8	6.4	6.1	0.0	0.1	0.3
No.200, 0.075 mm	3.8	3.5	3.0	0.0	0.0	0.0

The material for each replicate test was 2000 gm, and dry sieving test was done to determine the processed black curve. The sieve sizes used for this test were: 25 mm (1 inch), 19 mm (3/4 inch), 12.5 mm (1/2 inch), 9.5 mm (3/8 inch), 4.75 mm (No.4), 2.36 mm (No.8), 1.18 mm(No.16), 0.6mm (No.30), 0.3 mm (No. 50), 0.15 mm (No.100), and 0.075 mm (No.200). Even though RAP A of Mix 1 was fractioned, it still holds larger pieces compared to plain aggregates. After the ignition oven test, the RAP A of Mix 1 was sieved and the same sample weight and sieve size was used for the processed white curve. Figure 3.6 shows the three replicates of processed black curve and processed white curve of RAP A: Black Curve 1, 2, 3, and White Curve 1,2, and 3.

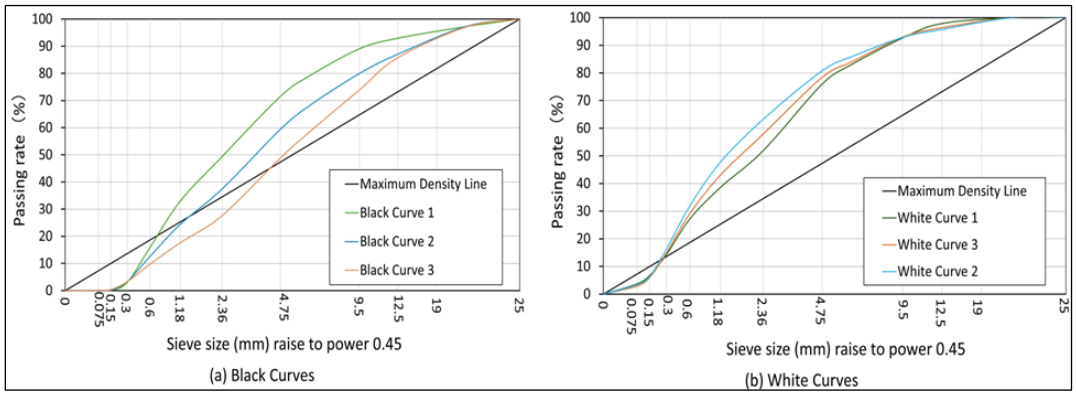

Figure 3.6 Processed Black and White Curves of RAP A of Mix 1.

The processed white curve is finer than the processed black curve because the binder holds together pieces of aggregates. As seen in Figure 3.6 (a), the Black Curve 1 has the higher passing rate at finer sieve sizes compared to the other two curves indicating a finer mix. Black Curve 3 is the coarsest amongst the three, as it has a lower passing rate at the finer sieve sizes. It can be observed that in black curve there is a distinct gradation difference between three replicates, whereas the white curves of the three replicate have identical gradation. This signifies that removing binder from the RAP material, results in identical gradation of replicate samples.

Figure 3.7 represents the chunk index value of Mix 1. The Black Curve 3 and White Curve 3 have high Chunk Index value of 92.3, compared to Black Curve 1, White Curve 1, and Black Curve 2, White Curve 2. As can be seen from Figure 3.6 (a) and (b) the Black Curve 3 was much coarser, while the White Curve 3 became significantly finer, which resulted in a high chunk index. Figure 3.7 (a) Chunk Index of Black Curve 1, White Curve 1 is 18.3, the lowest among the three-chunk index value. This suggests that although three replicate tests were conducted from the same box, the first replicate RAP contained more chunk than last replicate. This indicates that the top box had fewer RAP chunks compared to the bottom.

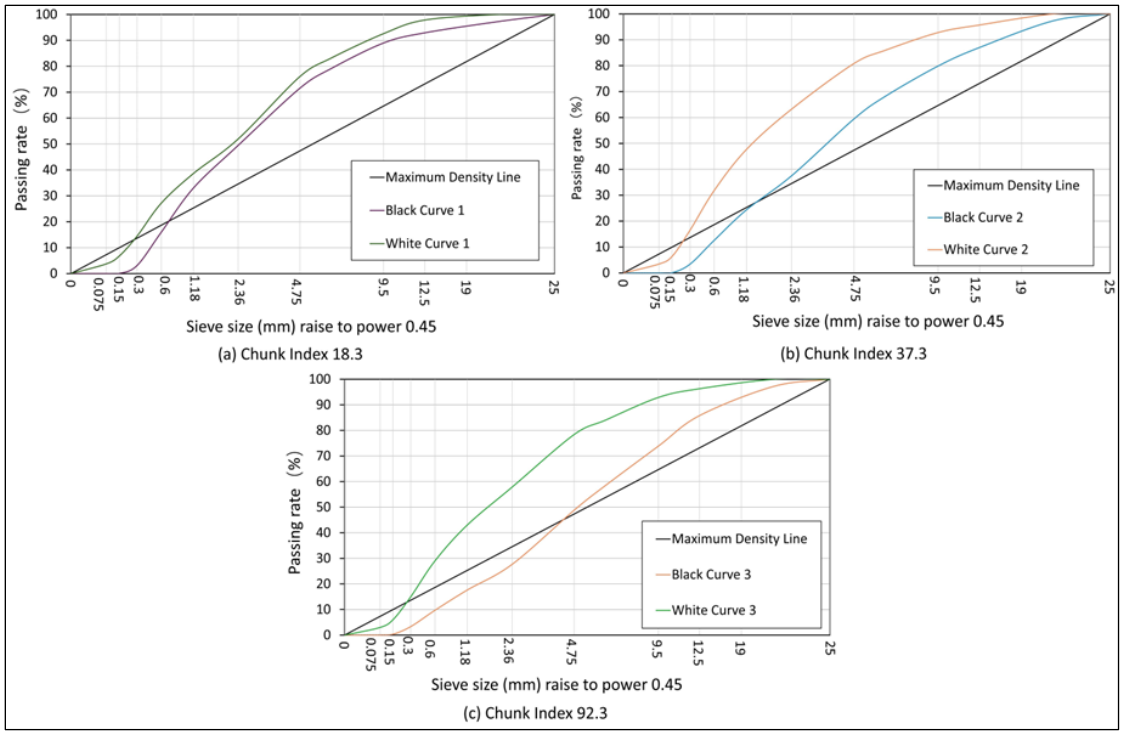

Figure 3.7 Chunk index of Mix 1.

3.3.3 Development of Mixture Design Spreadsheet

To determine how RAP content affects the compaction performance of asphalt mixtures, the research team attempted to obtain asphalt mixtures with almost identical aggregate gradations. For gradation

design, the gradation of RAP was considered using the white curves, which were obtained by ignition method. The final design gradation of asphalt mixtures with various content of RAP represented the combination of natural aggregates gradation and RAP gradation from the white curves. RAP was not sieved and divided into different classes or categories. For the total amount of binder in the mixture, it is assumed that it consists of aged binder introduced by RAP, as well as plain binder that will be added during mixing process. Regarding the activation of aged binder, the research team investigated two scenarios: a) 60% of the aged binder in RAP is activated and will combine with new binder, b) aged binder is 100% activated and will combine with new binder. In both scenarios, white curves of RAP were used for gradation design. In other words, the influence caused by inactivated aged binder on white curves was neglected.

For a target aggregate gradation, the designed gradation of natural aggregates and RAP should be as identical possible as the target gradation at each sieve size. This can be achieved by controlling the target function by the least square method, i.e.:

$$f_{\text{target}} = \min \sum_{\text{i}} \left(P_{\text{target}} - P_{\text{design}}\right)^2 \tag{3.3}$$

where, f_{target} is target function; i is the i^{th} sieve; P_{target} is the passing rate of the target aggregate gradation at the ith sieve size; P_{design} is the passing rate of the designed gradation at the ith sieve size. The target function is set to minimize the square of the difference between the passing rate of the target aggregate gradation and passing rate of the designed gradation summed over all the sieve sizes.

The research team developed a mixture design spreadsheet with SOLVER add-on. The spreadsheet consists of two parts, a data input table on the left and a gradation curve display on the right. Upper and lower limits are the gradation boundaries. The spreadsheet not only outputs a designed gradation at a certain RAP content, but also provides a material preparation list for laboratory compaction.

The design gradation of asphalt mixture with RAP can be obtained by the following steps:

- Step 1: Input gradation of natural aggregates and RAP. For natural aggregates, gradation should be input for each category. For RAP, white curve was adopted to represent the gradation.
- Step 2: Input RAP content for the designed mixture, e.g. 25%, 40%, and 50%.
- Step 3: Set constraints for the proportion of each aggregate category and RAP. This step helps to control the proportion of aggregates using certain restrictions on the percentage of aggregate categories.
- Step 4: Input aged binder content. The aged binder content is obtained by calculating the mass loss percentage using ignition method.

3.3.4 Mix Design

The four mixtures, designed using the raw materials from Mix 1, were labeled as follows: Superpave 5-total RAP content in the mixture-percent of activated aged binder-replicate sample. Each mixture had

two replicates, a, and b. For example, SP5-25-100%-a, denotes a Superpave 5 mixture with 25% RAP content with 100% activated aged binder, replicate 1.

The control mixture, comprising of 25% RAP, was based on the original mix design. The research team designed the gradation for 40% and 50% RAP mix by adopting the control mix design for fine aggregates, and using the spreadsheet mentioned in the previous section. The optimum binder content of 5.8% listed in the report was also adopted. Aggregate gradations are presented in Table 3.10, and mixture combinations design results are presented in Table 3.11 and Table 3.12.

Table 3.10 Aggregate gradation of mixtures with 25%, 40%, and 50% RAP contents.

Sieve size	Passing rate (%)		
	SP5-25-100% (Control Mix)	SP5-40-100% and SP5-40-60%	SP5-50-100%
1 in, 25mm	100	100	100
3/4 in, 19mm	100	100	100
1/2 in, 12.5mm	93.25	92.95	92.95
3/8 in, 9.5 mm	85.88	84.97	84.98
No.4, 4.75 mm	63.95	61.10	61.14
No.8, 2.36 mm	46.03	44.87	44.9
No.16, 1.18mm	34.04	33.82	33.83
No.30, 0.6mm	25.05	25.27	25.26
No.50, 0.3mm	15.21	15.46	15.45
No.100, 0.15mm	7.01	8.06	8.05
No.200, 0.075mm	3.99	4.93	4.92

Table 3.11 Bulk specific gravity and theoretical maximum specific gravity.

	SP5-25-100%	SP5-40-100%	SP5-40-60%	SP5-50-100%
Bulk Specific gravity (G_{mb})	2.433	2.445	2.446	2.450
Theoretical Maximum specific gravity (G_{mm})	2.463	2.455	2.455	2.466

Table 3.12 Mixture design.

	RAP content	Aged binder activation	Total binder content	Fresh binder content
SP5-25-100% (Control Mix)	25%	100%	5.8%	4.6%
SP5-40-100%	40%	100%	5.8%	3.72%
SP5-40-60%	40%	60%	5.8%	4.55%
SP5-50-100%	50%	100%	5.8%	3.2%

3.4 Compaction Experiments

3.4.1 Gyratory Compaction with 100 Gyrations

Gyratory compacted samples of 150 mm diameter were prepared at 100 gyrations. The aggregate and RAP A were pre-heated in the oven at 160℃ and 135℃ respectively. Subsequently, asphalt binder PG 58S-28 was added to the mixture and thoroughly mixed for 2 minutes. The asphalt mixtures were weighed and compacted in the Superpave Gyratory Compactor at 110℃.

Equation 3.4 is used to calculate the compacted asphalt mixture's air void content. Equations 3.5 and 3.6 are used to calculate bulk specific gravity (G_{mb}) and theoretical maximum specific gravity (G_{mm}), respectively.

$$\text{Air void content} = \left(\frac{G_{mb} - G_{mm}}{G_{mb}}\right) * 100 \tag{3.4}$$

where G_{mm} is the Theoretical Maximum Specific Gravity, and G_{mb} is the Bulk Specific Gravity. The air void content is equal to the relative difference between the bulk specific gravity and the theoretical maximum specific gravity with respect to the bulk specific gravity. The bulk specific gravity calculated by dividing the mass of the specimen in air by the difference between the mass of the surface-dry specimen in air and the mass of the specimen in water:

$$G_{mb} = \frac{E}{B - C} \tag{3.5}$$

where *E* is the mass in grams of the specimen in air, *B* is the mass in grams of the surface-dry specimen in air, and *C* is the mass in grams of the specimen in water. The theoretical maximum specific gravity is given by the ratio between the mass of oven-dry sample and the sum of the mass of oven-dry sample and the mass of container filled with water at 25 °C minus the mass of container filled with sample and water at 25 °C:

$$G_{mm} = A/(A + D - E) \tag{3.6}$$

where *A* is the mass of oven-dry sample in air, *D* is the mass of container filled with water at 25 °C, and *E* is the mass of container filled with sample and water at 25 °C.

3.4.2 Compaction Curves

Figure 3.8 represents the compaction curve of mixture with 25%, 40%, and 50% RAP content, assuming 100% activated binder in RAP. The Superpave 5 mixture with 50% RAP content assuming 100% activated

binder replicate 1 and 2, SP5-50-100% a and b reaches the target air void content 5% at 12 gyrations, The Superpave 5 mixture with 40% RAP content assuming 100% activated binder replicate 1 and 2, SP-40-100% a and b reaches the target air void content at 17 gyrations, while the Superpave 5 mixture with 25% RAP content assuming 100% activated binder replicate 1 and 2, SP-25-00% a and b reaches the target air void content 5% at 24 gyration. The results indicate that increasing the RAP-A content improves the compatibility of Mix 1.

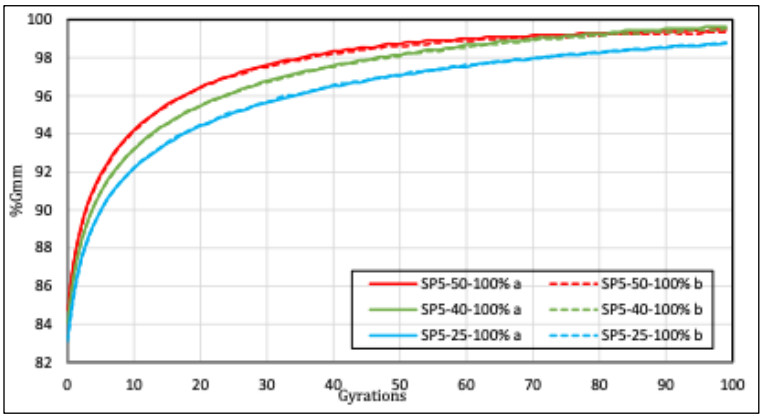

Figure 3.8 Compaction curves of Mix 1 with 25%, 40%, and 50% RAP contents.

Figure 3.9 represents the compaction curve of Superpave 5 mixture with 40% RAP content and comparing the characteristics of the mixture assuming 60%, and 100% activated binder in the RAP. The Superpave 5 mixture with 40% RAP content, assuming 60% activated binder in RAP replicate 1 and 2, SP5-40-60% a and b reached the target air void 5% at 8 gyrations, whereas the Superpave 5 mixture with 40% RAP content, assuming 100% activated binder in RAP replicate 1 and 2, SP5-40-100% a and b reached the target air void 5% at 17 gyrations. Although the compaction of SP5-40-60% reached the target air void with fewer gyrations than SP5-40-100%, its compaction remained constant beyond 40 gyrations. In contrast, the SP5-40-100% compacted steadily up to 99 gyrations. This suggests that assuming 60% activated binder, which requires adding more virgin binder, results in excess binder and bleeding in the asphalt mixture during the compaction test, indicating that mixture should be designed assuming 100% activated binder instead of 60%.

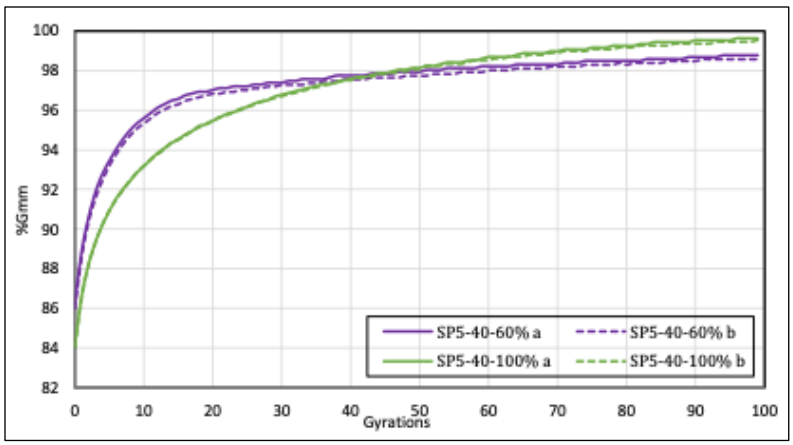

Figure 3.9 Compaction curves of Mix 1 SP5-40 with 100% and 60% active binder in RAP.

3.4.3 Compaction of Mixtures at the Target Air Void Content

The research team prepared a new set of samples, incorporating 25%, 40%, and 50% RAP content, each with three replicates, that were compacted to the target air void content. Figure 3.8 was used to determine the number of gyrations. The compaction results are shown in Figure 3.10. The RAP with 60% activated binder in the mixture was not used in the experiments. The mixture with 50% RAP content, assuming 100% activated binder, was the easiest to compact compared to the mixture, achieved the target air void of 5% between 4 and 6 gyrations, while the 40% and 25% RAP mixtures reached the target air void between 10 to 12 and 15 to 17 gyrations, respectively. This result could be caused by two reasons: 1) the RAP and the virgin mix have similar gradations, and 2) the RAP was heated to 135°, temperature at which the old binder separated from the aggregate. If the RAP particles were heated at a lower temperature, we may not expect that 100% of old binder from the RAP would be activated, which may affect the performance of the RAP mixture. The research team is currently investigating the effect of heating temperature of RAP on the compaction behavior of RAP mixture.

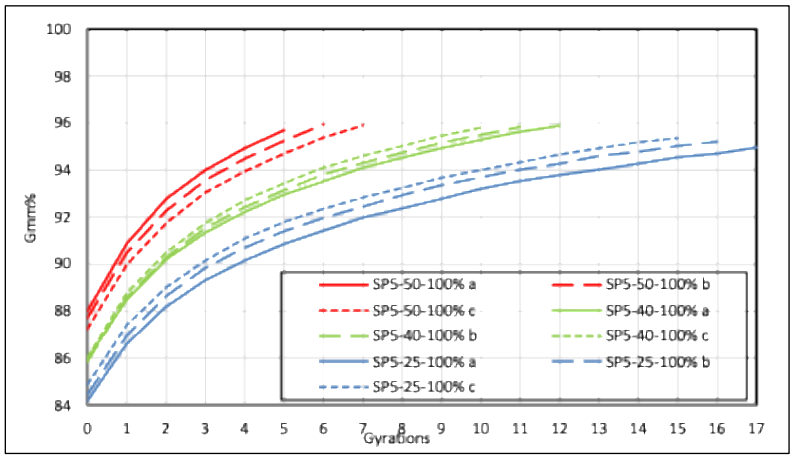

Figure 3.10 Compaction curves of Mix 1 reaching the target air void content.

Chapter 4: Compaction Performance of GNP Modified RAP Materials

This chapter discusses a set of gyratory compaction experiments on graphite nano-platelet (GNP) modified RAP materials. The research team investigated how the addition of GNP would affect the compaction performance of mixes prepared at different RAP heating temperatures and also compacted at different temperatures.

4.1 Background of GNP Modified Asphalt Materials

GNPs are produced from the exfoliated graphene, which has shown great mechanical and electron transport properties: the stiffness of graphene is in the order of 1TPa, the strength of graphene is about 100 times of that of steel, and the electric conductivity of graphene is somewhat higher than that of copper (Novoselov et al. 2005, Zhang et al. 2005, Lee et al. 2008). Furthermore, it has been shown that graphene has an exceptional thermal stability up to at least 2600K (Kim et al. 2010). The cost of GNP is much lower than that of carbon nanotubes (CNT).

In a series of studies, Le and Marasteanu explored the use of GNP materials to improve the mechanical properties of asphalt binders and mixtures (Le et al. 2019, Marasteanu et al. 2019). The authors showed that the addition of GNPs does not significantly affect the low-temperature relaxation properties of the binder as described by the *m*-value obtained in the bending beam rheometer creep test, and results in a small increase in creep stiffness. However, the addition of GNPs leads to a remarkable improvement in the flexural strength at low temperatures. For both plain and SBS-modified asphalt binders, a moderate addition of GNPs, i.e. 3% to 6% by weight of the binder, could result in a 130% increase in flexural strength. Such an increase has never been observed in other binder modifiers. It is also found that the strength improvement becomes less pronounced when a large amount of GNP addition is used. More research is needed to determine what mechanism is responsible for this effect.

In the same studies, the compaction experiments indicated that the addition of GNPs can lead to a 20–40% reduction in the number of compaction gyrations required to achieve a target air voids (Le et al. 2019). It is also found that, for some mix designs, the GNPs can also reduce the temperature dependence of the compaction process. This effect is similar to the effect observed in warm mix asphalt. The results indicate that the addition of GNPs could allow contractors to compact asphalt mixtures to higher densities from the beginning, which would improve the long-term durability and performance of asphalt pavements.

Motivated by the improvements in both mechanical and compaction properties of GNP-modified asphalt materials, in this task we investigated the compaction behavior of GNP-modified RAP material. In particular, we aim to understand whether adding GNP to the binder can offset incomplete RAP heating and still achieve adequate compaction.

4.2 Experimental Procedure

Asphalt mixtures containing more than 30–40 percent RAP typically requires heating up RAP at very high temperatures (around 280–300°C) in order to achieve binder mobilization. Failing to reach those temperatures would lead to poor coating, reduced workability, and substandard compaction. Our previous study (Le et al. 2019) has shown that GNP can enhance the thermal conductivity and rheological properties of asphalt binders leading to improved compaction performance. In this task, we added 6% of GNP (type 4827) by weight of the fresh binder, and considered different heating temperatures for RAP (105°C, 125°C, and 145°C) as well as different compaction temperatures (95°C, 115°C, and 135°C).

We reused the previously developed 50 percent RAP mix based on the virgin aggregate gradation and binder content of "Mix 1" (4.6% AC fresh) as described in Chapter 2. All samples share the same aggregate gradation and binder percentage; only the RAP heating temperature and the presence of GNP vary. As shown in Table 4.1, two mix designs were considered in this task. Both mixes used PG 58S-28 binder and 50% RAP content. One mix was prepared without GNP, and one with the addition of 6% GNP by weight of the fresh binder (the total weight would be 106% of the original binder weight). To evaluate the influence of GNP on the compaction performance of RAP, we prepared RAP at different heating temperatures. To isolate the effect of RAP heating temperature, we prepared the aggregates and binder in separate ovens before mixing. Table 4.2 summarizes the procedures for preparing the individual components of the RAP mixes.

Table 4.1 Mix design of RAP materials

	RAP content (%)	Binder type	GNP addition
Control mix	50	PG 58S-28	None
GNP modified mix	50	PG 58S-28	6% by weight of fresh binder

Table 4.2 Materials preparation for RAP materials with different RAP contents

Component	Oven temperature	Heating duration	Notes
Virgin aggregates mix	145°C	Overnight	Ensures full drying and thermal equilibration
Binder (virgin or GNP-modified)	145°C	Until temperature equilibration	GNP mixed manually into hot binder
RAP	105°C, 125°C, 145°C	Until the target temperature reached	Three sets of samples at each temperature

The detailed preparation procedure is described as follows:

- We placed a clean pan containing the virgin aggregates mix in a laboratory oven at 145°C and kept it overnight.
- Next day morning we put the binder in the same oven and removed it once the binder temperature reached 145°C.
- For the GNP-modified variant, we stirred 6 percent GNP (by mass of binder) into the hot binder until fully dispersed.
- We put the RAP in a separate oven pre-set to the designated heating temperature (105°C, 125°C, or 145°C). We constantly monitored the temperature until the RAP core reaches the preset heating temperature.
- We quickly mixed the hot virgin aggregates and binder (with or without GNP) in the mixing bowl, and added the preheated RAP. We blended everything for 2 minutes.
- After step 5, the temperature of the sample may drop during the mixing. Therefore, we put the mix back in the pan, and stored the pan for another 30 min in the oven at the compaction temperature.

As mentioned, for both control and GNP modified mixes, we considered three heating temperatures for RAP preparation. For each heating temperature, we compacted the specimen at a different temperature. Table 4.3 shows the heating and compaction temperatures for each RAP mix.

Table 4.3 RAP mixes for the compaction experiments

RAP mix ID	GNP	Heating temperature (°C)			Compaction temperature (°C)
		Aggregates	Binder	RAP	
135 NO	NONE	145	145	145	135
115 NO	NONE	145	145	125	115
95 NO	NONE	145	145	105	95
135 GNP	6% by wt	145	145	145	135
115 GNP	6% by wt	145	145	125	115
95 GNP	6% by wt	145	145	105	95

The gyration compaction experiments were performed on the six RAP mixes as listed in Table 4.3. For each mix, three replicates were tested. In the experiments, the initial height of the mix was set to be 110 mm, and the compaction was completed once the target compaction height was reached. The final target height corresponds to a 5% air void ratio. During the compaction process, we measured the evolution of specimen height, based on which we can estimate the average bulk density of the mixture at the *N*th gyration, $\rho_{ave}(N)$, by multiplying the final density of the compacted specimen with the ratio between the final height of the specimen and specimen height at the Nth gyration:

$$\rho_{ave}(N) = \rho_{ave}^{f} \frac{h^{f}}{h(N)} \tag{4.1}$$

where $h(N)$ is the specimen height at the Nth gyration, and h^f denotes the final height of the specimen. The average packing fraction of the specimen at the Nth gyration, ϕ_{ave}(N), can then be calculated as the ratio between the average bulk density of the mixture at the Nth gyration and the theoretical maximum density of the mixture:

$$\phi_{ave}(N) = \rho_{ave}(N)/\rho_m \quad (4.2)$$

where ρ_m is the theoretical maximum density of the mixture. By plotting the evolution of the average packing fraction, we obtained the compaction curve.

4.3 Measured Number of Gyrations for Reaching 5% Air Void Ratio

Table 4.4 shows the total number of gyrations of each specimen to reach the target 5% air void ratio. It is observed that, by comparing the control mix and the GNP modified mix, for a given heating and compaction temperatures, the addition of GNP improves the compaction performance, i.e. reduces the number of gyrations by 8%-16%. It is noted that this improvement is less significant than that observed for 6% GNP modification of asphalt mixtures without RAP (Le et al. 2019). This difference could be attributed to the fact that, in this study, we added 6% GNP by weight of the fresh binder. In the mix design, we assumed that, upon heating, 100% of old binder in the RAP is active, and would be completely mixed with the fresh binder. With the high RAP percentage, the actual amount of GNP added in this study is less than that added in the previous study.

Table 4.4 Number of gyrations to reach 5% air void ratio

Sample	Numer of gyrations at 5% air void ratio	Average number of gyrations
135 NO #1	21	18
135 NO #2	16	
135 NO #3	18	
135 GNP #1	14	15
135 GNP #2	16	
135 GNP #3	15	
115 NO #1	16	18
115 NO #1	18	
115 NO #1	20	
115 GNP #1	16	16
115 GNP #2	15	
115 GNP #3	16	
95 NO #1	28	25
95 NO #2	23	

95 NO #3	23	
95 GNP #1	26	23
95 GNP #2	23	
95 GNP #3	20	

It is seen from Table 4.4 that, for both control and GNP modified mixes, the number of gyrations is almost unchanged when we change the compaction temperature from 135°C to 115°C. However, when we further lower down the compaction temperature, the number of gyrations required for 5% air void ratio increases significantly. The addition of GNP does not lead to a significant decrease in gyration number that enables us to compact the RAP mix at significantly lower temperature (e.g. decrease from 135°C to 95°C). Nevertheless, it is seen that by adding GNP we could compact the RAP mix by using a somewhat lower heating and compaction temperature (decrease from 135°C to 115°C), leading to a less energy consumption for RAP preparation.

4.4 Compaction Curves

Figure 4.1a)-c) present the compaction curves for RAP mixes at 135°C, 115°C, and 95°C, respectively. It is seen from these figures that the effect of GNP on the compaction curves displays a similar trend for all different compaction temperatures. The addition of GNP does not affect the initial packing fraction prior to the gyration compaction as well as the overall shape of the compaction curve. However, clearly it has a positive effect on the rate of compaction over the entire compaction process. It is noted that the improvement in the compaction rate is more pronounced during the initial stage of the compaction. Such a phenomenon has also been observed in GNP modified asphalt mixtures (Le et al. 2019). To explain this trend, we note that the influence of GNP on the compaction performance of asphalt mixtures is because GNP alters the rheological properties of the binder (Marasteanu et al. 2019). During the initial stage, most aggregates do not contact each other, and the compaction behavior is primarily governed by the rheological behavior of the binder. This is why GNP modification has a pronounced effect. As the compaction proceeds, the aggregates are rearranged towards their optimum packing configuration and start to contact each other. In this case, the rheological behavior of the binder has less effect on the compaction rate.

In principle, the improvement we observed in this study could be further enhanced if we add more GNP to the fresh binder. However, mixing a large amount of GNP with fresh binder could lead to clustering of GNP particles. It might not be practically possible to add more than 10% GNP by weight of the fresh binder. This becomes a challenge if we want to further increase the RAP content. When the RAP content becomes large, we would add a smaller portion of fresh binder, which implies a smaller amount of GNP addition. Therefore, to effective use the GNP, there would be a maximum limit of RAP content we should use for the mix design unless we improve the procedure for mixing binder and GNP.

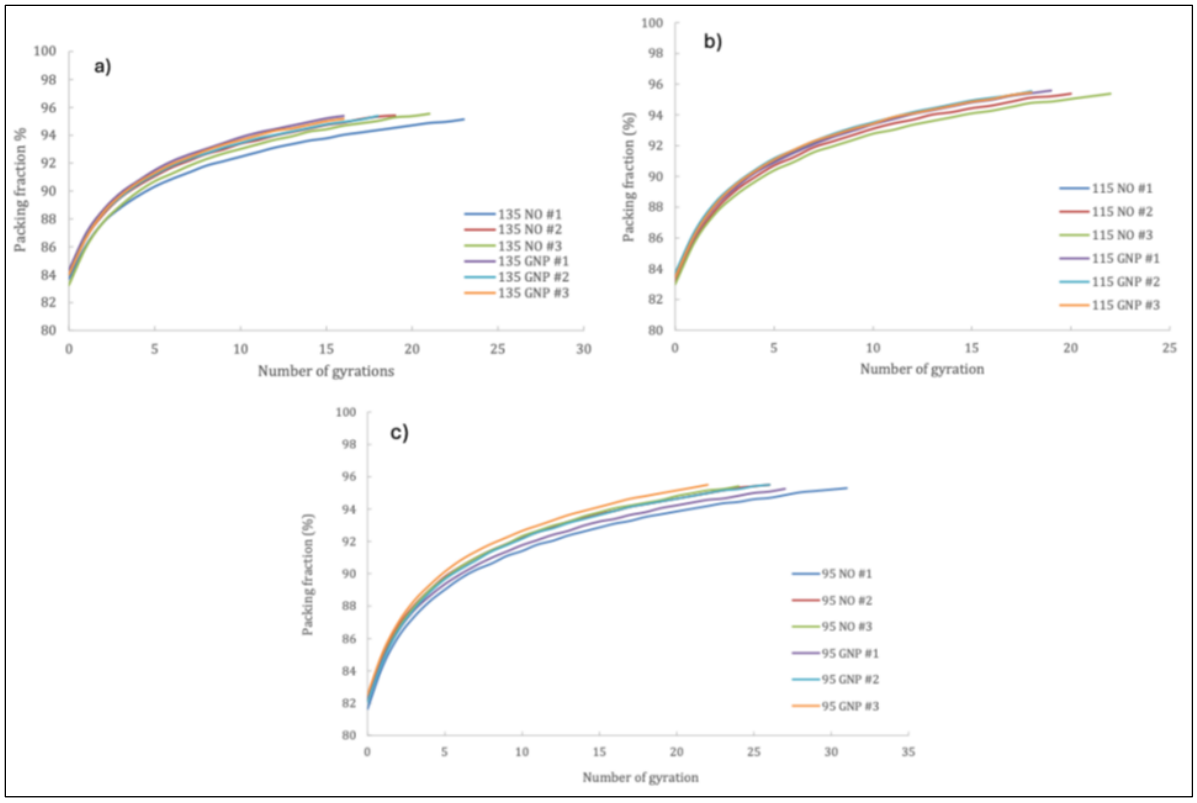

Figure 4.1 Compaction curves of RAP mixes at different temperatures: a) 135°C, b) 115°C, and c) 95°C.

Chapter 5: Strength and Fracture Experiments on RAP Mixtures

This chapter discusses the low-temperature bending beam rheometer (BBR) strength tests and semi-circular bend (SCB) fracture tests on the RAP materials. The objective is to evaluate the low-temperature fracture resistance of the RAP materials in conjunction with the compaction tests. In addition, the same strength and fracture tests are performed on a virgin mix with the same PG-grade binder and gradation curve, allowing the performance of the RAP materials to be directly compared with that of the virgin material.

5.1 Material Tests

Of the four mixtures developed in Chapter 3 using raw materials from Mix 1, three were selected for this task. The mixture designed with 60% activated aged binder was excluded due to its high binder content and the occurrence of bleeding during compaction.

The control mixture, containing 25% RAP, was prepared in accordance with the original mix design. For mixtures with 40% and 50% RAP contents, the fine aggregate portion of the control mix design was maintained, while the overall gradation was adjusted using the spreadsheet described in section 3.3.3 . In addition, a new virgin mixture, designated SP5-00-000%, was included for comparison. This mixture was designed using the same PG-grade binder source and a gradation curve similar to those of the RAP mixtures, and it contains 5.8% binder with no aged binder.

The four mixtures are summarized in Table 5.1. The volumetric properties and aggregate gradations of the mixtures are presented in Table 5.2 and Table 5.3, respectively.

Table 5.1 Asphalt mixture information

Mix	RAP, %	Activated aged binder, %
SP5-25-100%	25	100
SP5-40-100%	40	100
SP5-50-100%	50	100
SP5-00-000%	0	0

Table 5.2 Bulk specific gravity and theoretical maximum specific gravity

	SP5-25-100%	SP5-40-100%	SP5-50-100%	SP5-00-000%
Bulk Specific gravity (G_{mb})	2.433	2.445	2.450	2.355
Theoretical Maximum specific gravity (G_{mm})	2.463	2.455	2.466	2.40

Table 5.3 Aggregate gradations of mixtures with 0%, 25%, 40%, and 50% RAP

Sieve size	Passing rate (%)			
	SP5-25-100% (Control Mix)	SP5-40-100%	SP5-50-100%	SP5-00-000%
1 in, 25mm	100	100	100	100
3/4 in, 19mm	100	100	100	100
1/2 in, 12.5mm	93.25	92.95	92.95	92.5
3/8 in, 9.5 mm	85.88	84.97	84.98	83.86
No.4, 4.75 mm	63.95	61.10	61.14	63.89
No.8, 2.36 mm	46.03	44.87	44.9	47.19
No.16, 1.18mm	34.04	33.82	33.83	34.22
No.30, 0.6mm	25.05	25.27	25.26	24.97
No.50, 0.3mm	15.21	15.46	15.45	11.41
No.100, 0.15mm	7.01	8.06	8.05	5.24
No.200, 0.075mm	3.99	4.93	4.92	2.61

It was observed that the SP5-00-000% mix contains a smaller proportion of fines compared with the other mixtures, despite using the same gradation optimization tool. This difference can be attributed to the fact that RAP typically contains a higher fraction of fines due to the reclamation process.

Figure 5.1 shows the compaction curves for mixtures with varying RAP contents (0%, 25%, 40%, and 50%). In the mix design, the RAP binder was assumed to be 100% activated. The two replicates of the Superpave 5 mixture containing 50% RAP reached the target air void content of 5% at 12 gyrations. The mixture with 40% RAP reached the same target at 17 gyrations, while the 25% RAP mixture reached it at 24 gyrations. In contrast, the virgin mixture without RAP (SP5-00-000%) required 40 gyrations to achieve 5% air voids. These results indicate that increasing the RAP content enhances the compactability of Mix 1.

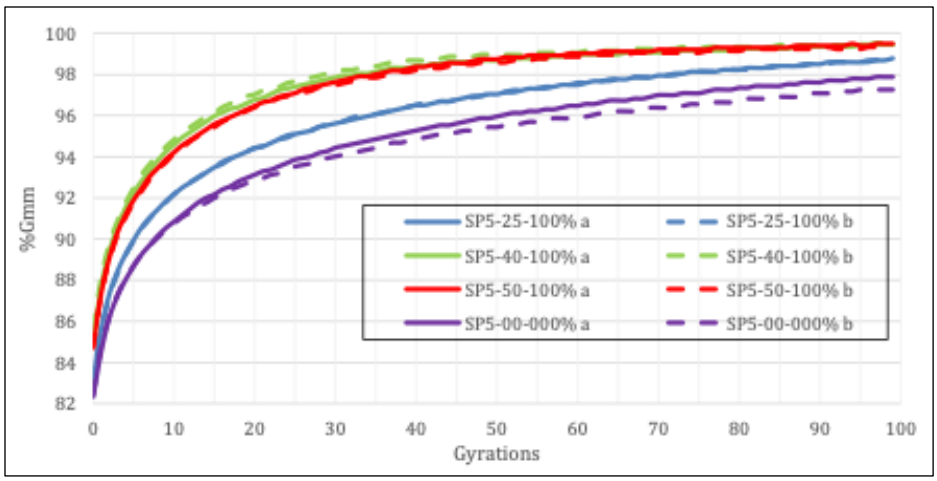

Figure 5.1 Comparison curves of the four mixtures.

The observed difference in the compaction behavior between the RAP mixes and virgin mixes can be explained as follows:

- Clean virgin aggregates are uncoated, which requires greater effort for particle rearrangement and interlock during compaction. In contrast, RAP aggregates are pre-coated with aged binder, reducing friction and facilitating the rapid formation of a dense aggregate skeleton.
- Virgin mixes have thicker binder films that act as a cushion, delaying direct aggregate contact and increasing the number of gyrations required to reach the target air voids. In RAP mixes, a portion of the binder remains locked within the RAP particles, resulting in thinner effective binder films, earlier aggregate contact, and fewer gyrations needed for compaction.
- As shown in Table 5.3, RAP contains a higher proportion of fines and angular particles, which enhances interlock and reduces voids.

5.2 Experimental Testing Program

To evaluate low-temperature fracture resistance, two testing methods were employed: Bending Beam Rheometer (BBR) testing for creep and strength, and low-temperature semi-circular bend (SCB) fracture testing. Cylindrical specimens were prepared from compacted mixtures for both tests, as summarized in Table 5.4.

All cylindrical specimens were compacted at the University of Minnesota Pavement Lab to a height of 150 mm and a target air void content of 5%. From each cylinder, a 12.5 mm slice was taken for BBR testing, and a 32 mm slice was used for SCB testing. The SCB slices were then split into two semicircular specimens, each featuring a 15 mm-long, 1 mm-wide notch centered perpendicular to the diameter. One semicircular specimen was tested at −18 °C, and the other at −28 °C.

Table 5.4 Specimen preparation for asphalt mixtures used in the experimental work

Test	Number of specimens per mixture	Testing Temperatures and Number of Replicates
BBR mixture creep and strength	12 beams	Six tested at -28°C (creep, recovery, strength) Six tested at -18°C (creep, recovery, strength)
SCB	6 semicircular slices	Three tested at -28°C and three tested at -18°C

5.2.1 Semi-circular Bending Tests

Semi-Circular Bending (SCB) fracture tests were conducted in accordance with AASHTO TP-105 (AASHTO 2018). All mixtures were tested at both temperatures using three replicates. The fracture energy measured by the SCB test is a material property that directly represents the fracture resistance under mode-I loading (tensile fracture). The work of fracture is determined as the area under the loading-deflection (*P-u*) curve. The average fracture energy G_f can then be obtained by dividing the work of fracture with the ligament area, where the work is equal to the integral of force-displacement curve:

$$G_f = \frac{\int Pdu}{A_l} \tag{5.1}$$

Where $\int Pdu$ is the total work done by the external force *P*, and A_l is the ligament area. Equation 5.1 assumes that the external work is all spent in crack propagation and the rest part of the specimen behaves elastically.

The apparent fracture toughness can also be calculated from the measured peak load of the specimen within the framework of linear elastic fracture mechanics (LEFM). The essential failure criterion of LEFM is that the stress intensity factor (SIF) of the specimen reaches a critical value (i.e. fracture toughness) as the peak load is attained. The SIF of the SCB specimen can be written by:

$$K = \frac{P}{2rt}\sqrt{\pi a}\left\{4.782 + 1.219\left(\frac{a}{r}\right) + 0.063exp\left[7.045\left(\frac{a}{r}\right)\right]\right\} \tag{5.2}$$

where *r* is radius of the SCB specimen, *t* is the thickness of specimen, and *a* is the notch depth. Considering the LEFM failure criterion, we can compute the fracture toughness K_{1c} based on Equation 5.2 from the experimentally measured peak load. It should be emphasized here that the fracture toughness computed by Equation 5.2 is strictly anchored by the assumption of LEFM. For SCB specimen, it has been shown that the LFEM limit may not be achieved since the fracture process zone at the crack

tip is not necessarily negligible compared to the specimen size (Le et al. 2013, Li and Marasteanu 2004, Lim et al. 1993). Therefore, the research team refer this calculated K_{1c} as to the apparent fracture toughness. The true fracture toughness is the value of K_{1c} for an infinite size specimen, which is a material property. By contrast, the apparent fracture toughness strongly depends on specimen geometry and size, and therefore it does not directly measure the actual fracture resistance of the material.

Table 5.5 summarizes the calculated fracture energy and apparent fracture toughness for all specimens, while Figure 5.2 presents fracture energy and Figure 5.3 shows apparent fracture toughness. As noted previously, apparent fracture toughness is not an intrinsic material property but depends on the specimen size relative to the fracture process zone. Interestingly, all mixes exhibit similar fracture energy, yet the apparent fracture toughness of the virgin mix (SP5-00-000%) is noticeably lower than that of the RAP mixes. According to size effect theory, for the given specimen geometry, a smaller fracture process zone leads to more brittle behavior and a lower peak load. These results indicate that the virgin mix is more brittle than the RAP-containing mixtures.

Table 5.5 Fracture energy and apparent fracture toughness

Mix	Fracture Energy, G_f (kJ/m2)		Fracture Toughness, K_{IC} (MPa*m0.5)	
	-18°C	-28°C	-18°C	-28°C
SP5-00-000%	0.301	0.197	0.590	0.617
SP5-25-100%	0.276	0.226	0.790	0.794
SP5-40-100%	0.337	0.235	0.738	0.745
SP5-50-000%	0.310	0.206	0.794	0.767

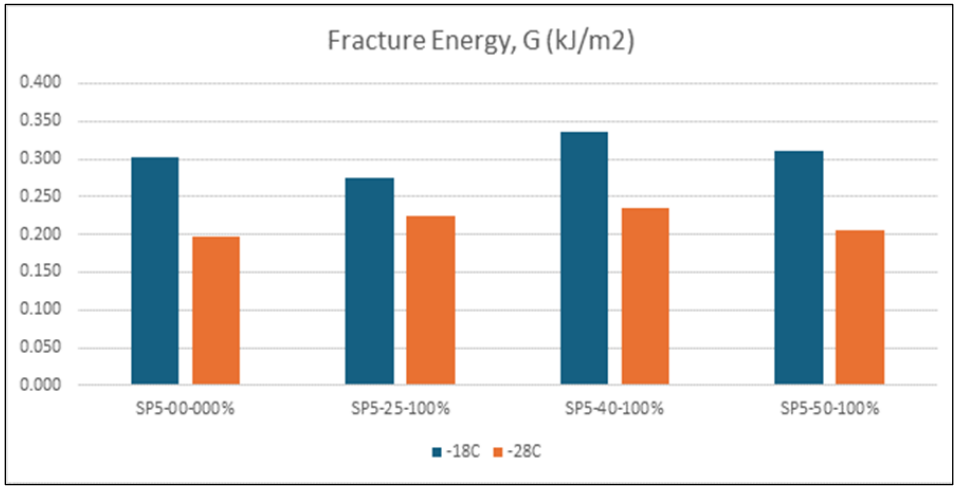

Figure 5.2 Measured fracture energies for all mixtures.

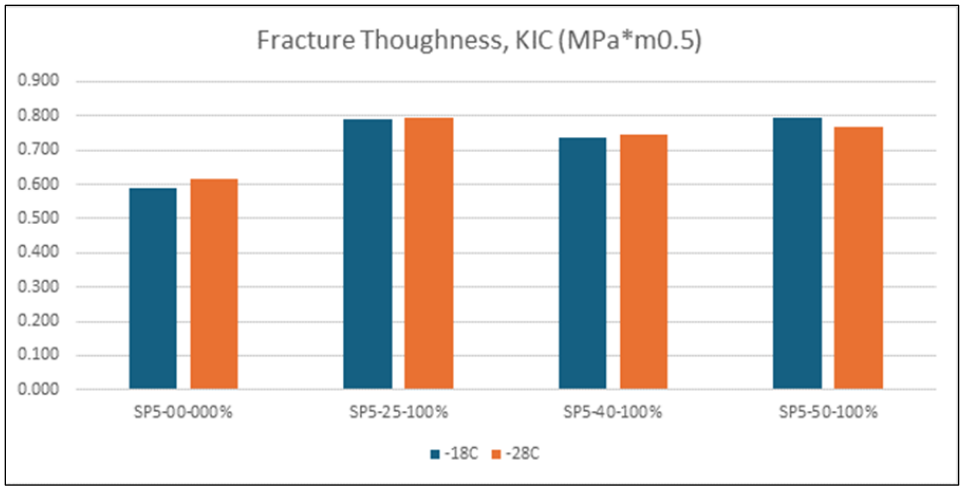

Figure 5.3 Measured fracture toughness for all mixtures.

5.2.2 Bending Beam Rheometer (BBR) Tests

For the BBR testing, specimen preparation followed the procedure described in Task 4a. Each mixture beam was tested using a combined protocol consisting of an initial BBR creep test [68], a recovery period, and a subsequent strength test (Marasteanu 2012) without removing the beam from the testing frame. Creep tests were performed for 1000 seconds, allowing results from different temperatures to overlap when shifted to construct master curves. Tests were conducted at −18 °C and −28 °C for each mixture, with six replicates per condition. The highest and lowest strength values (outliers) were discarded, and the average was calculated from the remaining four specimens.

To accommodate the small deflections typical of mixture testing, the creep loads were set at 6 N and 8 N for −18 °C and −28 °C, respectively. Following creep, a 60-second recovery period was applied using a minimal seating load to measure recovery deflection. After recovery, a strength test was performed with a constant loading rate chosen to reach 44 N within 1 minute. The test continued until beam failure.

A summary of the BBR creep results at 60 s is presented in Figure 5.4 and Figure 5.5 and Table 5.6, while BBR strength and failure strain results are shown in Table 5.7.

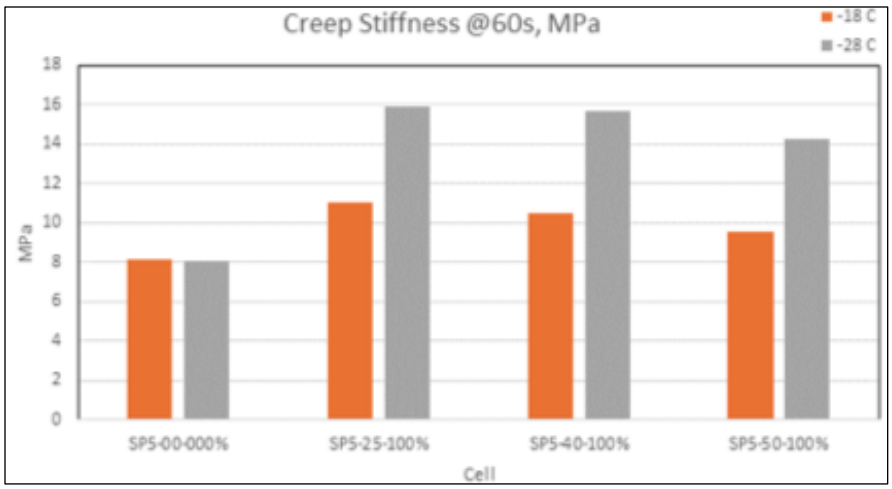

Figure 5.4 BBR mixture creep stiffness at 60 seconds.

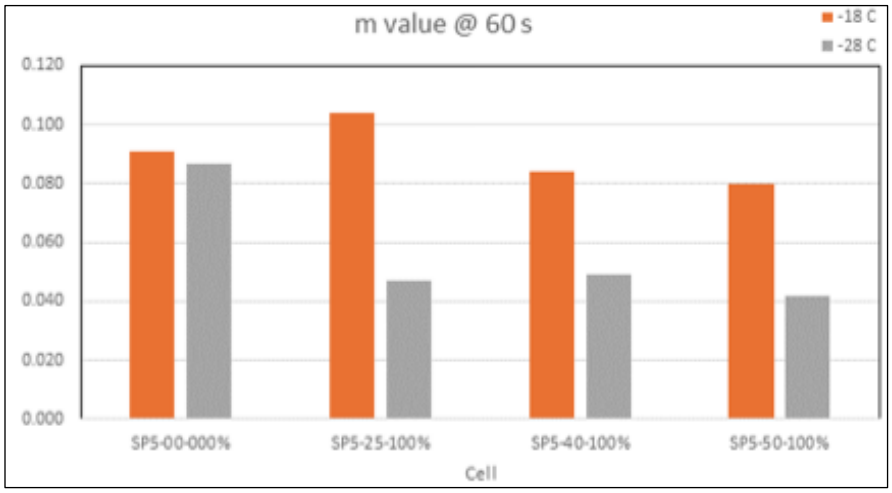

Figure 5.5 BBR *m*-values at 60 seconds.

Table 5.6 BBR creep stiffness and *m*-values

Mix	Temperature °C	S(60s) MPa	CV %	m(60s)	CV %	Max. Deflection, mm	CV %
SP5-00-000%	-18	8.116	17	0.091	17	0.055	11
	-28	8.050	5	0.087	18	0.080	8
SP5-25-100%	-18	11.046	7	0.104	6	0.046	12
	-28	15.900	8	0.047	13	0.042	10
SP5-40-100%	-18	10.514	18	0.084	8	0.041	16
	-28	15.705	28	0.049	9	0.041	10
SP5-50-100%	-18	9.563	10	0.080	11	0.043	10
	-28	14.301	11	0.042	18	0.038	8

Table 5.7 Failure stresses and strains, and failure loads measured in BBR tests

Mix	Temperature °C	Stress @ Failure, MPa	CV %	Strain @ Failure, %	CV %	Load @ Failure, N	CV %
SP5-00-000%	-18	7.8	14	0.065	28	26.4	19
	-28	6.0	9	0.036	23	20.2	9
SP5-25-100%	-18	10.5	7	0.074	8	32.4	8
	-28	8.6	10	0.038	7	25.7	7
SP5-40-100%	-18	10.9	10	0.076	13	36.6	13
	-28	8.3	21	0.042	13	26.6	10
SP5-50-100%	-18	11.4	5	0.078	8	38.6	7
	-28	8.9	17	0.047	14	29.9	17

5.2.3 Statistical Analysis of BBR Test Results

In this analysis, independent two sample t-tests were conducted to compare performance metrics among the different mixtures based on BBR results. The t-test is a widely used statistical method for determining whether the means of two groups differ significantly. For this study, the mean values of strength, creep stiffness (S), and m-value—obtained from six replicates at two temperatures—were analyzed. This method is particularly suitable for small sample sizes and situations where the population standard deviation is unknown.

The independent two-sample t-test was applied under the following assumptions:

- Data is approximately normally distributed.
- Samples are independent.
- Variances are equal across groups.

A p-value < 0.05 indicates a statistically significant difference between group means. Table 8 presents the t-test results for BBR strengths of the virgin mix and the 25% RAP mix (SP5-00-000% vs. SP5-25-100%), showing a statistically significant difference. Table 5.8 summarizes t-test results for all BBR metrics (strength, creep stiffness, and m-value) across all mixtures at −18 °C and −28 °C. In Table 5.8, green cells denote p-values > 0.05, indicating no statistically significant difference, while white cells denote p-values < 0.05, indicating a statistically significant difference.

Table 5.9 summarizes the t-test results by showing the number of BBR properties that exhibit significant and non-significant differences for each pair of mixtures. Based on the number of tests with p-values below and above 0.05, the virgin mixture (SP5-00-000%) differs from all RAP-containing mixtures, including the original design (SP5-25-100%), in 5 out of 6 comparisons. In contrast, almost all comparisons among RAP-containing mixtures show no statistically significant differences.

Table 5.8 Summary of *p*-value for the *t*-test on different BBR results

Mixtures	*t*-test for strength at -18 °C			Mixtures	*t*-test for strength at -28 ° C		
	SP5-0-0%	SP5-25-100%	SP5-40-100%		SP5-0-0%	SP5-25-100%	SP5-40-100%
SP5-0-0%	0.00038	0.00015	0.00005	SP5-0-0%	0.00004	0.00817	0.00024
SP5-25-100%		0.23902	0.10466	SP5-25-100%		0.77508	0.45406
SP5-40-100%			0.75760	SP5-40-100%			0.44753
Mixtures	*t*-test for stiffness at -18 ° C			Mixtures	*t*-test for stiffness at -28 ° C		
	SP5-0-0%	SP5-25-100%	SP5-40-100%		SP5-0-0%	SP5-25-100%	SP5-40-100%
SP5-0-0%	0.00109	0.00764	0.03224	SP5-0-0%	0.000003	0.00039	0.00006
SP5-25-100%		0.70384	0.10606	SP5-25-100%		0.83745	0.19006
SP5-40-100%			0.29186	SP5-40-100%			0.48389
Mixtures	*t*-test for *m*-value at -18 °C			Mixtures	*t*-test for *m*-value at -28 °C		
	SP5-0-0%	SP5-25-100%	SP5-40-100%		SP5-0-0%	SP5-25-100%	SP5-40-100%
SP5-0-0%	0.96906	0.26979	0.15325	SP5-0-0%	0.00542	0.00307	0.00618
SP5-25-100%		0.01164	0.00331	SP5-25-100%		0.67551	0.70784
SP5-40-100%			0.17803	SP5-40-100%			0.54069

Table 5.9 Number of tests with and without significant differences

Mix 1	Mix 2	Number of tests	
		Statistically significant difference	NO statistically significant difference
SP-00-000%	SP-25-100%	5	1
SP-00-000%	SP-40-100%	5	1
SP-00-000%	SP-50-100%	5	1
SP-25-100%	SP-40-100%	1	5
SP-25-100%	SP-50-100%	1	5
SP-40-100%	SP-50-100%	0	6

Chapter 6: Summary, Conclusions, and Recommendations

In this chapter, the research team summarized the work completed in this study and presented the main conclusions and recommendations related to RAP mixture design, compaction behavior, GNP modification, and low-temperature mechanical performance. Recommendations for future research and for the practical evaluation of high-RAP mixtures are also provided.

6.1 Summary

This project investigated the mix design, compaction behavior, and low-temperature mechanical performance of recycled asphalt pavement (RAP) mixtures, with additional evaluation of graphite nanoplatelet (GNP) modification. The study was motivated by the increasing use of RAP in asphalt pavements and the need to better understand not only the mechanical properties of RAP mixtures but also their compaction behavior, which strongly affects pavement durability and field performance.

The work began with a literature review on asphalt mixture compactability, factors affecting compaction, and previous research on RAP mixtures. Particular attention was given to binder viscosity, binder lubrication, aggregate gradation, aggregate characteristics, and the use of gradation-based design approaches such as the Bailey method. The review also examined prior studies on high-RAP mixtures, fractionated RAP, and methods used to characterize RAP processing quality, including the processed black curve, processed white curve, and chunk index.

The experimental phase first focused on RAP characterization and conventional RAP mixture design. Several RAP sources were evaluated using ignition oven testing and sieve analysis. Their processed black and white curves were compared, and chunk indices were used to assess the degree of RAP agglomeration and the suitability of the materials for mix design. Based on this evaluation, the raw materials and the mix design for a Superpave 5 mixture used in a paving project on TH 30 (Mix 1), were selected for a detailed investigation. A mix design spreadsheet was developed to determine the proportions of virgin aggregates and RAP needed to produce target gradations for mixtures with different RAP contents. Using this approach, mixtures containing 25%, 40%, and 50% RAP were prepared and tested in the gyratory compactor. The results showed that, under the laboratory preparation conditions used in this study, mixtures with higher RAP contents were easier to compact and reached the target air void content with fewer gyrations. The study also compared assumptions of 100% and 60% activated aged binder and found that the 60% activation assumption required additional virgin binder and resulted in bleeding, indicating excess binder in the mixture.

The second phase of the study examined the compaction performance of GNP-modified RAP mixtures. A 50% RAP mixture was selected and prepared with and without 6% GNP by weight of fresh binder. RAP heating temperatures of 105°C, 125°C, and 145°C were considered together with compaction temperatures of 95°C, 115°C, and 135°C. Gyratory compaction results showed that GNP improved compaction performance by reducing the number of gyrations required to reach 5% air voids. The

results also showed that for both control and GNP-modified mixtures, reducing compaction temperature from 135°C to 115°C caused little change in gyration demand, whereas further reduction to 95°C caused a substantial increase. These findings suggest that GNP can help improve compactability and may support some reduction in heating and compaction temperatures, although the effect is limited in high-RAP mixtures when the fresh binder fraction is relatively small.

The final phase of the project focused on the low-temperature strength, fracture, and creep performance of RAP mixtures. Semi-circular bend (SCB) fracture tests and bending beam rheometer (BBR) mixture tests were conducted on mixtures containing 0%, 25%, 40%, and 50% RAP. The results showed that the RAP mixtures had fracture energies similar to those of the virgin mixture, but higher apparent fracture toughness and higher flexural strength. Statistical analysis of the BBR results indicated that the virgin mixture differed from the RAP mixtures in most comparisons, while differences among the RAP mixtures themselves were generally not statistically significant. Overall, the results indicated that, under the assumptions and laboratory conditions used in this study, increasing RAP content did not negatively affect low-temperature mechanical performance.

6.2 Conclusions and Recommendations

This research investigation has shown that RAP mixtures can be successfully designed and evaluated using a combination of RAP characterization, gradation-based mixture design, compaction analysis, and low-temperature mechanical testing. Within the materials and laboratory conditions considered in this project, increasing RAP content did not reduce compactability or low-temperature performance, and the addition of GNP provided a moderate improvement in compaction behavior. These findings support the continued use and further investigation of higher-RAP mixtures, while also highlighting the importance of RAP processing quality, binder activation assumptions, and mixture production conditions. The following conclusions were drawn:

- Characterization of RAP using processed black and white curves together with the chunk index was effective for evaluating RAP processing quality and suitability for mixture design. A lower chunk index indicated fewer RAP particle agglomerates and a more homogeneous material, which supports more consistent blending with virgin aggregates and binder. In contrast, a higher chunk index suggested stronger agglomeration and greater risk of mixture variability. Therefore, these parameters provided useful information beyond binder content and gradation alone and can help identify RAP materials that are more suitable for higher-percentage use in asphalt mixtures.
- Under the laboratory conditions used in this study, increasing RAP content improved compactability, and the 50% RAP mixture performed best. The 50% RAP mixture reached 5% air voids in fewer gyrations than the 40% and 25% RAP mixtures. Because the mixtures had nearly identical aggregate gradations, this improvement was likely due to the greater contribution of mobilized RAP binder under the selected heating and mixing conditions. The additional effective binder likely improved lubrication between aggregate particles and reduced resistance to densification during compaction.

- For the tested 40% RAP mixture, the assumption that only 60% of the aged RAP binder was activated resulted in excessive virgin binder addition and caused bleeding during compaction. This indicated that the 60% activation assumption overestimated the amount of virgin binder required under the laboratory conditions used in this study and produced an unstable mixture. The result also suggested that binder activation in RAP mixtures may have been higher than assumed, likely because the laboratory heating and mixing conditions allowed more aged binder to become mobilized and blend with the new binder, and contribute to the overall binder phase.
- The addition of GNP to the fresh binder improved the compaction performance of RAP mixtures, and reduced the number of gyrations required to achieve the target air void content. However, the benefit was moderate compared with previous results for mixtures without RAP, because the GNP dosage was based only on the fresh binder portion and therefore became effectively smaller as RAP content increased.
- For both control and GNP-modified 50% RAP mixtures, lowering the compaction temperature from 135°C to 115°C caused little change in the number of gyrations needed to reach 5% air voids. In contrast, lowering the compaction temperature further to 95°C significantly increased gyration demand. This indicates that moderate temperature reduction may be feasible, but larger temperature reductions substantially reduce compactability.
- The SCB and BBR results showed that the RAP mixtures had low-temperature mechanical properties comparable to, and in some respects better than, the virgin mixture tested in this study. Fracture energy remained similar across mixtures, while RAP mixtures showed higher apparent fracture toughness and higher flexural strength than the virgin mixture.
- Statistical analysis showed that the virgin mixture differed from the RAP mixtures in most BBR comparisons, while differences among the RAP mixtures themselves were generally not statistically significant. This suggested that, within the range of 25% to 50% RAP evaluated in this study, increasing RAP content did not produce major differences in low-temperature creep and strength behavior.

Additional research is needed to improve RAP characterization, refine mixture design assumptions, and further evaluate the role of GNP in high-RAP mixtures. A few simple steps can be provided at this time:

- The assumption regarding the degree of aged binder activation should be further investigated. In this study, the assumption of 60% activation led to excess virgin binder and bleeding, while the 100% activation assumption was more consistent with the observed compaction behavior under the selected heating conditions. Additional work is needed to quantify binder activation as a function of RAP source, heating temperature, mixing procedure, and mixing duration.
- GNP modification should continue to be studied as a potential means of improving compactability, especially for mixtures produced at reduced temperatures. Future work should examine alternative dosage strategies, including dosage relative to total active binder rather than fresh binder only, and should also consider practical issues related to GNP dispersion and clustering.
- Additional research should investigate the effect of RAP heating process on binder mobilization and compaction performance. This research demonstrates, one more time, that the heating

temperature and duration strongly influence the extent of aged binder activation, and represent a critical issue and obstacle for practical application of high-RAP mixtures.

- Field validation is recommended to confirm whether the laboratory trends observed in this report, particularly the improved compactability at higher RAP contents and the moderate benefit of GNP, translate to plant production and field compaction conditions.

In conclusion, the limited results obtained in this study indicate that adding more RAP decreases the compaction effort to reach target air voids, which is contrary to expectations. Possible explanations are:

- Sufficient heat is provided to RAP particles to “activate” all aged binder.
- Coated RAP particles are less angular and coated with a film of activated binder that makes it easier to compact.
- RAP fine particles are rich in binder and may aid packing at early stages, if binder is fully activated.

This trend is not observed in the field, and most likely this is due to the mismatch between laboratory fabrication conditions and the asphalt mix plant conditions, where the heating and mixing times are very short. In the asphalt mix plant, adding more RAP requires longer heating times to activate the RAP binder, considerably slowing down production and increasing energy costs. Aggregates can be superheated, but there are limits to it, and it can negatively affect aging of the binder during mixing.

Preheating of RAP particles can solve the problem, but requires extra costs associated with better technologies such as using an additional drum or using a microwave system to heat RAP particles.

Further research is needed to investigate the laboratory procedure for preparing asphalt mixtures with high RAP content. The current procedure does not match the current production conditions in a conventional mixing plant.

References

AASHTO. (2018). *AASHTO TP 125-16: Methods of test for determining the flexural creep stiffness of asphalt mixtures using the bending beam rheometer (BBR)*. AASHTO.

Anderson, R. (2002). *Relationship of Superpave gyratory compaction properties to HMA rutting behavior* (Vol. 478). Transportation Research Board.

ASTM. (2006). *ASTM C136-06: Standard test method for sieve analysis of fine and coarse aggregates*. West Conshohocken. ASTM International.

Bahia, H., Fahim., A, & Nam, K. (2006). Prediction of compaction temperatures using binder rheology. In *Proceedings of the 84th Annual Meeting*, 3–17

Bahia, H., & Paye, B. (2001). *Minimum pavement lift thickness for Superpave mixtures* (WHRP 03-02). Wisconsin Department of Transportation.

Canestrari, F., Ingrassia, L., Ferrotti, G., & Lu, X. (2017). State of the art of tribological tests for bituminous binders. *Construction and Building Materials, 157*, 718–728.

Copeland, A. (2011). *Reclaimed asphalt pavement in asphalt mixtures: State of the practice* (Publication No. FHWA-HRT-11-021). Federal Highway Administration.

D'Angelo, S., Cardone, F., Spadoni, S., De Santis, F., & Canestrari, F. (2024). Laboratory Investigation and in-plant production validation of dense-graded warm mixtures with reclaimed asphalt. *Proceedings of ICONFBMP*, 2024.

Dessouky, S. (2015). Laboratory and field evaluation of asphalt concrete mixture workability and compactability. *Proceedings of Airfield and Highway Pavements 2015,* Edited by J., Harvey and K. F. Chou, 97–106.

Ding, Y., Huang, B., & Shu, X. (2016). Characterizing blending efficiency of plant produced asphalt paving mixtures containing high RAP*. Construction and Building Materials, 126*, 172–178.

Finn, F., & Epps, J. (1980). *Compaction of hot mix asphalt concrete*. Texas Transportation Institute, Texas A & M University System.

Graziani, A., Ferrotti, G., Pasquini, E., & Canestrari, F. (2012). An application to the European practice of the Bailey method for HMA aggregate grading design. *Procedia - Social and Behavioral Sciences*, *53,* 990-999.

Gudimettla, J., Cooley, L., & Brown, E. (2003). *Workability of hot mix asphalt* (NCAT Report 03-03). National Center for Asphalt Technology.

Guler, M., Bahia, H., Bosscher, P., & Plesha, M. (2000). Device for measuring shear resistance of hot-mix asphalt in gyratory compactor. *Transportation Research Record, 1723*(1), 116–124.

Hanz, A., & Bahia, H. (2013). Asphalt binder contribution to mixture workability and application of asphalt lubricity test to estimate compactability temperatures for warm-mix asphalt. *Transportation Research Record, 2371,* 87–95.

Hekmatfar, A., McDaniel, R., Shah, A., & Haddock, J. (2015). *Optimizing laboratory mixture design as it relates to field compaction to improve asphalt mixture durability* (FHWA/IN/JTRP-2015/25). Indiana Department of Transportation.

Hesami, E., Jelagin, D., Kringos, N., & Birgisson, B. (2012). An empirical framework for determining asphalt mastic viscosity as a function of mineral filler concentration. *Construction and Building Materials, 35,* 23–29.

Huber, G., Haddock, J., Wielinski, J., Kriech, A., & Hekmatfar, A. (2016). Adjusting design air void levels in Superpave mixtures to enhance durability. In *Proceedings of the 6th Eurasphalt and Eurobitume Congress*.

Ingrassia, L., Lu, X., Canestrari, F., & Ferrotti, G. (2018). Tribological characterization of bituminous binders with warm mix asphalt additives. *Construction and Building Materials, 172,* 309–318.

Johnson, E., Watson, E., & Clyne, T. (2012). *MnROAD study of rap and fractionated RAP* (Research project final report 2012-39). Office of Materials and Road Research, Minnesota Department of Transportation.

Kallas, B., Puzinauskas, V., & Krieger, H. (1962). Mineral fillers in asphalt paving mixtures. *Highway Research Board Bulletin*, *329*.

Kataware, A., & Singh, D. (2018). Effects of wax-based, chemical-based, and water-based warm-mix additives on mechanical performance of asphalt binders. *Journal of Materials in Civil Engineering, 30*(10), 4018237.

Khatri, A., Bahia, H., & Hanson, D. (2001). Mixing and compaction temperatures for modified binders using the Superpave gyratory compactor. *Journal of the Association of Asphalt Paving Technologists, 70,* 368–402.

Kim, K., Regan, W., Geng, B., Aleman, B., Kessler, B., Wang, F., Crommie, M., & Zettl, A. (2011). High-temperature stability of suspended single-layer graphene. *Physica Status Solidi (RRL) – Rapid Research Letters*, 2011.

Le, J.-L., Cannone Falchetto, A., & Marasteanu, M. (2013). Determination of strength distribution of quasibrittle structures from size effect analysis. *Mechanics of Materials, 66,* 79–87.

Le, J.-L., Marasteanu, M., & Turos, M. (2019). Mechanical and compaction properties of graphite nano-platelet-modified asphalt binders and mixtures. *Road Materials and Pavement Design, 21,* (7), 1799–1814.

Leiva, F., & West, R. (2008). Analysis of hot-mix asphalt lab compactability using lab compaction parameters and mix characteristics. *Transportation Research Record, 2057*(1), 89–98.

Li, X., & Marasteanu, M. (2004). Evaluation of low temperature fracture resistance of asphalt mixtures using the semi-circular bend test. *Journal of the Association of Asphalt Paving Technologists, 73*, 401–426.

Lim, I., Johnson, I., & Choi, S. (1993). Stress intensity factor for semi-circular specimen under three-point bending. *Engineering Fracture Mechanics, 44*(3), 363–382.

Linden, R. N., Mahoney, J., & Jackson, N. (1989). Effect of compaction on asphalt concrete performance. *Transportation Research Record, 1217*.

Lo Presti, D., Vasconcelos, K., Oreskovic, M., Megegusso Pires, G., & Bressi, S. (2019). On the degree of binder activity of reclaimed asphalt and degree of blending with recycling agents. *Road Materials and Pavement Design, 21,* 1–20.

Marasteanu, M., Cannone Falchetto, A., Turos, M., & Le, J.-L. (2012). *Development* of a simple test to determine low-temperature strength of asphalt mixtures and binders (NCHRP-IDEA report 151). Transportation Research Board of the National Academies.

Marasteanu, M., Le, J. -L., Hill, K., Yan, T., Turos, M., Barman, M., Arepalli, U., & Munch, J. (2019). *Experimental and computational investigations of high-density asphalt mixtures* (MnDOT technical report MN/RC 2019-41). MnDOT.

MnDOT. (2018). *Minnesota Department of Transportation: Standard specifications for construction*. MnDOT.

MnDOT. (2020). *Minnesota Department of Transportation: Standard specifications for construction*. MnDOT.

MnDOT. (2016). *Minnesota Department of Transportation: Synopsis of recycled asphalt pavement (RAP) material* (Report no. MN/RC-2016RIC08). MnDOT.

Mo, L., Li, X., Fang, X., Huurman, M., & Wu, S. (2012). Laboratory investigation of compaction characteristics and performance of warm mix asphalt containing chemical additives. *Construction and Building Materials, 37,* 239–247.

Moutier, F. (1974). La Presse a cisaillement giratoire—Modele de serie. *Bulletin de Liaison des Laboratoires des Ponts et Chaussees*, *74.*

Newcomb, D., Epps, J., & Zhou, F. (2016). *Use of RAP & RAS in high binder replacement asphalt mixtures: A synthesis* (NAPA special report 213). National Asphalt Pavement Association.

Novoselov, K., Geim, A., Morozov, S., Jiang, D., Katsnelson, M., Grigorieva, I., Dubonos, S., & Firsov, A. (2005). Two-dimensional gas of massless dirac fermions in graphene. *Nature, 438,* 197.

Pine, W. (1997). *Superpave gyratory compaction and the Ndesign table*. Illinois Department of Transportation.

Sefidmazgi, N., Tashman, L., & Bahia, H. (2012). Internal structure characterization of asphalt mixtures for rutting performance using imaging analysis. *Road Materials and Pavement Design, 13*(1), 21–37.

Shamsi, K., & Mohammad, L. (2010). Estimating optimum compaction level for dense-graded hot-mix asphalt mixtures. *The Journal of Engineering Research, 7*(1), 11–21.

Shenoy, A. (2001). Determination of the temperature for mixing aggregates with polymer-modified asphalts. *International Journal of Pavement Engineering, 2*(1), 33–47.

Sreeram, A., Leng, Z., Zhang, Y., & Padhan, R. (2018). Evaluation of RAP binder mobilization and blending efficiency in bituminous mixtures: An approach using ATR-FTIR and artificial aggregate. *Construction and Building Materials, 179,* 245–253.

Stakston, A., & Bahia, H. (2003). *The effect of fine aggregate angularity, asphalt content and performance graded asphalts on hot mix asphalt performance*. Wisconsin Highway Research Program.

Stakston, A., Bahia, H., & Bushek, J. (2002). Effect of fine aggregate angularity on compaction and shearing resistance of asphalt mixtures. *Transportation Research Record, 1789*, 14–24.

Stimilli, A., Canestrari, F., Teymourpour, P., & Bahia, H. (2015a). Low-temperature mechanics of hot recycled mixtures through asphalt thermal cracking analyzer (ATCA). *Construction and Building Materials, 84*, 54–65.

Stimilli, A., Ferrotti, G., Radicioni, D., & Canestrari, F. (2015b). Performance evaluation of hot recycled mixtures containing SBS modified binder. In *Proceedings of the 6th ICONFBMP*.

Tang, Y., & Haddock, J. (2006). Field testing of the zero-shear viscosity method. *Factors Affecting Compaction of Asphalt Pavements, Transportation Research Circular*, 18–26.

Tarsi, G., Tataranni, P., & Sangiorgi, C. (2020). The challenges of using reclaimed asphalt pavement for new asphalt mixtures: A review. *Materials, 13*(18), 4052.

Vavrik, W., & Carpenter, S. (1998). Calculating air voids at specified number of gyrations in Superpave gyratory compactor. *Transportation Research Record, 1630*(1), 117–125.

Vavrik, W., Huber, G., Pine, W., Carpenter, S., & Bailey, R. (2002). Bailey method for gradation selection in hot-mix asphalt mixture design. *Transportation Research E-Circular*. Transportation Research Board.

Vivar, E., & Haddock, J. (2006). *HMA pavement performance and durability* (Report no. FHWA/IN/JTRP-2005/14). Indiana Department of Transportation and Purdue University.

Wang, H., Al-Qadi, I., Faheem, A., Bahia, H., Yang, S., & Reinke, G. (2011). Effect of mineral filler characteristics on asphalt mastic and mixture rutting potential. *Transportation Research Record, 2208*(1), 33–39.

West, R., Rodezno, C., Leiva, F., & Taylor, A. (2018). *Regressing air voids for balanced HMA mix design* (WHRP 0092-16-06). National Center for Asphalt Technology.

Willoughby, K., & Mahoney, J. (2007). *An assessment of WSDOT's hot-mix asphalt quality control and assurance requirements* (Report no. WA-RD 517.2). Washington State Department of Transportation.

Yan, T., Cash, K., Turos, M., & Marasteanu, M. (2023). High-compactability asphalt mix design framework based on binary aggregate packing. *Construction and Building Materials, 383,* 131315.

Yan, T., Ingrassia, L., Kumar, R., Turos, M., Canestrari, F., Lu, X., & Marasteanu, M. (2020). Evaluation of graphite nano-particles influence on the compaction properties of asphalt mixtures. *Materials, 13*(3).

Yan, T., Marasteanu, M., Le, J.-L., Turos, M., & Cash, K. (2022). *Development of Superpave 5 asphalt mix designs for Minnesota pavements (Report no. MN2022-18).* Minnesota Department of Transportation.

Yeung, E., Braham, A., & Barnat, J. (2016). Exploring the effect of asphalt-concrete fabrication and compaction location on six compaction metrics. *Journal of Materials in Civil Engineering, 28*(12), 04016163.

Yildirim, Y., Ideker, J., & Hazlett, D. (2006). Evaluation of viscosity values for mixing and compaction temperatures. *Journal of Materials in Civil Engineering, 18*(4), 545–553.

Yildirim, Y., Solaimanian, M., & Kennedy, T. (2000). Mixing and compaction temperatures for Superpave mixes. *Asphalt Paving Technology, 69,* 34–71.

Zaumanis, M., Boesiger, L., Kunz, N., Mazzoni, H., Bruhin, P., Mazora, S., & Poulikakos, L. (2022). Three indexes to characterize crushing and screening of reclaimed asphalt pavement. *International Journal of Pavement Engineering, 23*(14), 4977–4990.

Zaumanis, M., Loetscher, D., Mazor, S., Stöckli, F., & Poulikakos, L. (2021). Impact of milling machine parameters on the properties of reclaimed asphalt pavement. *Construction and Building Materials, 307*, 125114.

Zaumanis, M., & Mallick, R. (2013). Finite element modeling of rejuvenator diffusion in rap binder film—simulation of plant mixing process. *Multi-Scale Modeling and Characterization of Infrastructure Materials, 8*, 407–419.

Zhang, Y., Tan, Y., Stormer, H., & Kim, P. (2005). Experimental observation of the quantum hall effect and Berry's phase in graphene. *Nature, 438*, 201.